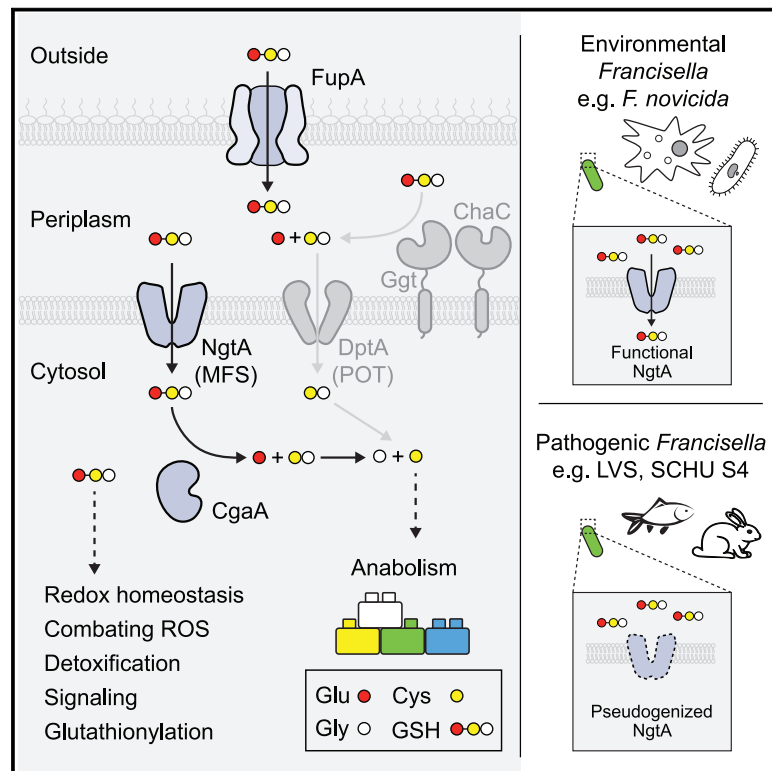


Cell Host & Microbe

Discovery of a glutathione utilization pathway in *Francisella* that shows functional divergence between environmental and pathogenic species

Graphical abstract



Authors

Yaxi Wang, Hannah E. Ledvina, Catherine A. Tower, ..., S. Brook Peterson, Jean Celli, Joseph D. Mougous

Correspondence

mougous@uw.edu

In brief

Host glutathione (GSH) is a source of cysteine during intracellular replication of *Francisella*. Wang et al. find *Francisella* imports GSH via a previously unknown transporter and discover a cytoplasmic GSH-degrading enzyme. This pathway is functional in non-pathogenic *Francisella* but pseudogenized in pathogenic lineages, suggesting its importance in an environmental niche.

Highlights

- Tn-seq identifies a previously unrecognized GSH utilization pathway in *F. novicida*
- A major facilitator transporter pseudogenized in pathogenic *Francisella* imports GSH
- *Francisella* uses a glutamine amidotransferase to degrade cytoplasmic GSH
- A single porin mediates the bulk of outer membrane GSH transport in *Francisella*

Article

Discovery of a glutathione utilization pathway in *Francisella* that shows functional divergence between environmental and pathogenic species

Yaxi Wang,¹ Hannah E. Ledvina,¹ Catherine A. Tower,¹ Stanimir Kambarev,² Elizabeth Liu,¹ James C. Charity,³ Lieselotte S.M. Kreuk,¹ Qing Tang,¹ Qiwen Chen,¹ Larry A. Gallagher,¹ Matthew C. Radey,¹ Guilhem F. Rerolle,⁴ Yaqiao Li,^{1,5} Kelsi M. Penewit,⁶ Serdar Turkarslan,⁵ Shawn J. Skerrett,⁴ Stephen J. Salipante,⁶ Nitin S. Baliga,⁵ Joshua J. Woodward,¹ Simon L. Dove,³ S. Brook Peterson,¹ Jean Celli,^{2,9} and Joseph D. Mougous^{1,7,8,10,*}

¹Department of Microbiology, University of Washington, Seattle, WA 98109, USA

²Paul G. Allen School for Global Health, Washington State University, Pullman, WA 99164, USA

³Division of Infectious Diseases, Boston Children's Hospital, Harvard Medical School, Boston, MA 02115, USA

⁴Department of Medicine, University of Washington, Seattle, WA 98195, USA

⁵Institute for Systems Biology, Seattle, WA 98109, USA

⁶Department of Laboratory Medicine and Pathology, University of Washington, Seattle, WA 98195, USA

⁷Microbial Interactions and Microbiome Center, University of Washington, Seattle, WA 98195, USA

⁸Howard Hughes Medical Institute, University of Washington, Seattle, WA 98109, USA

⁹Present address: Department of Microbiology and Molecular Genetics, Larner College of Medicine at the University of Vermont, Burlington, VT 05405, USA

¹⁰Lead contact

*Correspondence: mougous@uw.edu

<https://doi.org/10.1016/j.chom.2023.06.010>

SUMMARY

Glutathione (GSH) is an abundant metabolite within eukaryotic cells that can act as a signal, a nutrient source, or serve in a redox capacity for intracellular bacterial pathogens. For *Francisella*, GSH is thought to be a critical *in vivo* source of cysteine; however, the cellular pathways permitting GSH utilization by *Francisella* differ between strains and have remained poorly understood. Using genetic screening, we discovered a unique pathway for GSH utilization in *Francisella*. Whereas prior work suggested GSH catabolism initiates in the periplasm, the pathway we define consists of a major facilitator superfamily (MFS) member that transports intact GSH and a previously unrecognized bacterial cytoplasmic enzyme that catalyzes the first step of GSH degradation. Interestingly, we find that the transporter gene for this pathway is pseudogenized in pathogenic *Francisella*, explaining phenotypic discrepancies in GSH utilization among *Francisella* spp. and revealing a critical role for GSH in the environmental niche of these bacteria.

INTRODUCTION

It is increasingly appreciated that the success of bacterial pathogens relies on sophisticated strategies for scavenging nutrients from their hosts. These “nutritional virulence factors” can include mechanisms for manipulating the host to drive nutrient availability.¹ For example, some intracellular pathogens hijack autophagic or proteolytic cellular machinery to release amino acids that can be exploited as carbon and energy sources.^{2,3} Other pathogens compete effectively with the host for nutrients that are available as a result of normal host physiology.

One metabolite present in particularly high abundance inside host cells is the tripeptide glutathione (γ -L-glutamyl-L-cysteinyl-glycine, GSH). GSH and its oxidized counterpart GSSG play crucial roles in multiple essential processes, including maintaining redox homeostasis, defense against reactive oxygen species, and protein iron-sulfur cluster synthesis.⁴ Perhaps as

a result of the ubiquity and high concentration of GSH in the cytosol of eukaryotic cells, certain intracellular pathogens couple GSH sensing to virulence factor induction.⁵ Notable examples include *Burkholderia pseudomallei*, which induces type VI secretion transcription following GSH sensing by the VirAG two-component system, and *Listeria monocytogenes*, which senses GSH through PrfA, leading to the activation of a set of critical virulence determinants.^{6,7} Other pathogens, including *Hemophilus influenzae* and *Streptococcus* spp., rely on co-opted host GSH to defend against oxidative stress.^{8,9}

In contrast to these pathogens, Gram-negative proteobacteria belonging to the genus *Francisella* are sulfur amino acid auxotrophs and catabolize host GSH as a source of organic sulfur. A transposon screen of *Francisella tularensis* subspecies *holarctica* LVS (*F. tularensis* LVS) revealed that the periplasmic enzyme γ -glutamyl transpeptidase (GGT), which cleaves GSH into glutamate and cysteine-glycine (Cys-Gly), is essential for intracellular

replication of this organism.¹⁰ Using a similar approach, our laboratory identified an inner membrane proton-dependent oligopeptide transporter-family (POT) protein that imports Cys-Gly.¹¹ We named this protein DptA and demonstrated that, consistent with its critical role in GSH catabolism, *F. tularensis* LVS $\Delta dptA$ is defective in intracellular replication. However, we found that inactivation of *ggt* or *dptA* neither attenuates intracellular growth nor compromises GSH catabolism in a closely related *Francisella* strain, *F. tularensis* subsp. *novicida* (*F. novicida*). Rather, we identified a predicted γ -glutamylcyclo-transferase enzyme in *F. novicida*, ChaC, which participates in GSH catabolism and is required for robust *F. novicida* growth in media containing GSH as the sole organic sulfur source (GSH media).

Despite these additions to our understanding of GSH metabolism in *Francisella*, two lines of evidence suggested that it remained incomplete. First, if GSH breakdown by Ggt and ChaC represented the only entry points into GSH catabolic pathways in *F. novicida*, a strain lacking these enzymes should be unable to grow in media containing GSH as a sole cysteine source. On the contrary, we found that *F. novicida* Δggt $\Delta chaC$ grows in such media, albeit not at wild-type levels.¹¹ Second, although *ggt*, *dptA*, and *chaC* are present and expected to be functional in both *F. novicida* and *F. tularensis* LVS, inactivation of *ggt* only produces a growth defect in GSH media in *F. tularensis* LVS. Together, these observations led us to hypothesize that additional pathways for GSH catabolism remain to be uncovered in *Francisella*.

In this study, we employed transposon sequencing (Tn-seq) to identify Ggt-independent pathways important for GSH utilization in *Francisella*. Through this analysis, we discovered that *F. novicida* possesses a previously unrecognized pathway for GSH utilization that consists of an outer membrane porin, an inner membrane transporter of intact GSH belonging to the major facilitator superfamily (MFS), and a cytoplasmic glutamine amidotransferase (GATase) family enzyme capable of initiating degradation of the molecule. We show that this pathway is mutationally inactivated in pathogenic *Francisella* spp. but widely conserved in members of the genus that are believed to inhabit an environmental niche. Our work thus has implications for the evolution of pathogenesis within *Francisella* and provides evidence that the natural lifecycle of non-pathogenic *Francisella* likely includes replication within a GSH-rich habitat, such as the cytosol of unicellular eukaryotes.

RESULTS

Tn-seq reveals genes required for GSH utilization in *F. novicida* U112

Although Ggt is required for the growth of *F. tularensis* LVS in GSH medium, we previously found that its inactivation does not similarly impede *F. novicida* growth on this substrate.¹¹ Moreover, using the genome of *F. novicida*, we were unable to identify additional characterized GSH catabolism pathways that are absent from *F. tularensis* LVS. This conundrum motivated us to undertake an unbiased approach for discovering GSH catabolism pathways in *F. novicida*. To this end, we generated transposon mutant libraries of *F. novicida* in the wild-type and Δggt backgrounds and used transposon mutant sequencing

to compare gene insertion frequencies for each library grown in media containing GSH versus cysteine as the sole sulfur source (Figures 1A–1C). Our decision to employ Δggt rather than $\Delta chaC$ in this experiment was motivated by our recent observation that although *ggt* is not required for *F. novicida* growth when GSH is in excess (100 μ M), the growth yield of the Δggt strain is slightly reduced when the concentration of GSH limits growth (Figure S1). Strains lacking $\Delta chaC$ grow to wild-type levels under both conditions, suggesting that Ggt has a larger role in GSH catabolism in our *in vitro* culturing conditions.

Our Tn-seq screen led to the identification of many genes important for the growth of *F. novicida* Δggt specifically in GSH media. Among the 40 top hits in the Δggt background—corresponding to a 3-fold insertion frequency difference between cysteine and GSH as the sole sulfur source—only five were shared with wild type (Tables S1 and S2). Interestingly, although important for growth in GSH media specifically in the Δggt background, *chaC* was not among the strongest hits we observed (Table S2), supporting our earlier observation that Δggt $\Delta chaC$ can propagate in GSH media. Also consistent with our prior findings in the wild-type strain, the fitness cost of inactivating *ggt* or *dptA* in GSH media was modest (Figure 1B).

To highlight Ggt-independent pathways for GSH catabolism, we ranked *F. novicida* genes by the strength of their synthetic (Δggt versus wild type) growth phenotype in GSH media. Two genes ranked substantially higher in this analysis than other hits from our screen: FTN_1011 and FTN_0435 (Figure 1D). These two genes were also those with the greatest difference in insertion frequency between growth on GSH and cysteine as sole sulfur sources in the Δggt background (46.7- and 29.6-fold difference in normalized read counts, respectively) (Figure 1C; Table S2). Neither of these genes have been characterized nor have functions been ascribed to any close homologs. Thus, we hypothesized they could contribute to GSH catabolism through previously unknown mechanisms.

Identification and characterization of GSH transporter NgmA

The strongest synthetic phenotype during growth in GSH medium belonged to open reading frame FTN_1011—herein named *ngmA* (*novicida* GSH transporter A). NgmA is a member of the MFS of transporters, and as is typical of these proteins, its predicted structure displays 12 transmembrane helices organized into two six-helix bundles connected by a flexible linker.¹² Within the MFS, NgmA was previously classified into the Pht family.¹³ Interestingly, Pht family members are found exclusively in intracellular pathogens, and in *Legionella pneumophila* and *Francisella*, proteins in the family are important for intracellular replication by virtue of their role in amino acid transport or nucleoside transport.^{13–17} However, the sequence of NgmA is substantially divergent from characterized Pht family members (26% sequence identity shared with PhtA, the most closely related characterized Pht family member), and its function and substrate are unknown.

We hypothesized that NgmA could be a transporter of GSH. To test this hypothesis, we first generated in-frame deletion mutants of *ngmA* in the *F. novicida* wild-type and Δggt backgrounds. As predicted by our Tn-seq results, inactivation of *ngmA* in the wild-type background did not affect *F. novicida* growth in GSH medium (Figure 2A). However, growth of *F. novicida* Δggt $\Delta ngmA$

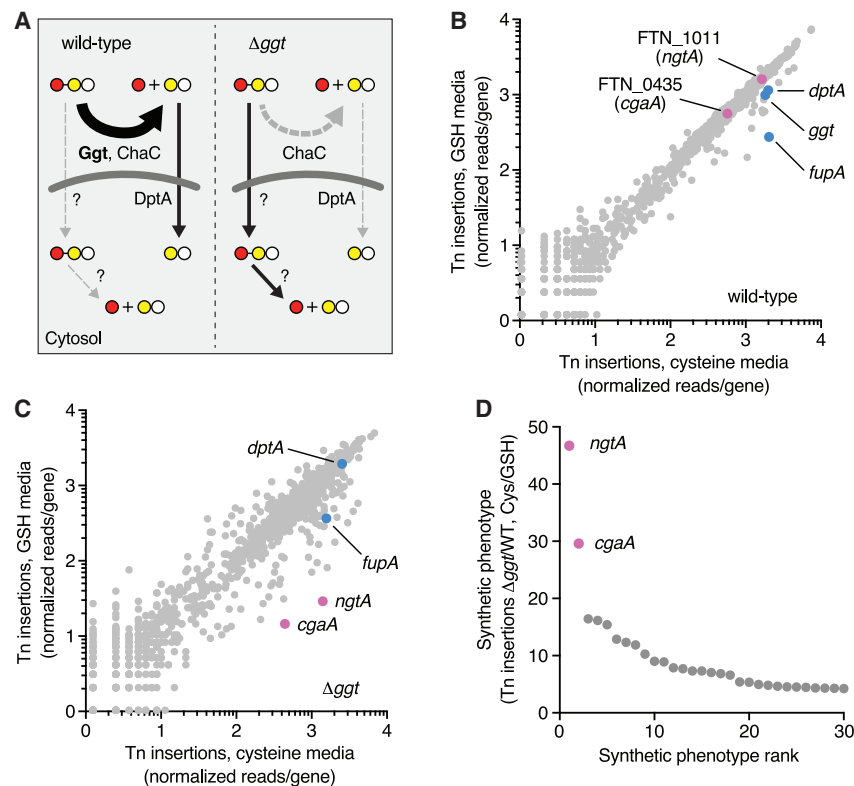


Figure 1. Tn-seq for discovery of *F. novicida* genes with synthetic phenotypes during growth on GSH

(A) Schematic illustrating known and unidentified potential GSH catabolism pathways and their products (Glu, red circle; Cys-Gly, yellow and white circles) in the two genetic backgrounds employed in our screen. The heavy arrow depicted for the wild-type background emphasizes the primary conversion pathway (left, Ggt-mediated), while the dashed arrow indicates the residual GSH cleavage mediated by ChaC in the absence of Ggt (right).

(B and C) Results of Tn-seq screen to identify genes required for growth of *F. novicida* on GSH medium in the wild-type (B) and Δggt backgrounds (C). Genes with the greatest difference in transposon insertion reads between growth in GSH and cysteine media in the wild-type (B) and Δggt backgrounds (C) are indicated.

(D) Rank order depiction of the strength of the synthetic phenotype for genes important for growth of *F. novicida* Δggt in GSH medium. Rank order was calculated by dividing the ratio of transposon insertion frequency obtained for each gene during growth on GSH compared with growth on cysteine using the *F. novicida* Δggt background by the same ratio obtained using the wild-type background. See also Figure S1 and Tables S1 and S2.

was strongly impaired in GSH medium. This growth defect could be complemented by repairing the deletion of *ngtA* via allelic exchange, and inactivation of *ngtA* did not cause growth defects in media containing cysteine as a sole sulfur source in either background (Figure S2A). To determine whether NgtA contributes to GSH uptake in *F. novicida*, we mixed cysteine-starved strains with ^3H -GSH ([Glycine-2- ^3H]-GSH) and measured cell-associated radiolabel following a short incubation (Figure 2B). In the wild-type strain, NgtA inactivation had no impact on ^3H -GSH transport. Because Ggt and ChaC generate periplasmic Cys-Gly, which, when transported into the cytoplasm by DptA, would mask the potential role of NgtA in intact GSH transport, we next employed the $\Delta ggt \Delta chaC$ background in these assays. As expected, these mutations diminished GSH transport; however, uptake of the labeled substrate dropped to levels approaching the limit of detection in *F. novicida* $\Delta ggt \Delta chaC \Delta ngtA$ (Figure S2B). This result supports the hypothesis that in the absence of GSH cleavage in the periplasm, the intact tripeptide can be transported to the cytoplasm via NgtA.

Our data left open the formal possibility that *F. novicida* possesses a third mechanism to generate Cys-Gly from GSH and that the dipeptide is the transport substrate of NgtA. Notably, our laboratory previously reported the *F. novicida* Cys-Gly transporter DptA.¹¹ This strain exhibits only a partial growth defect in media containing Cys-Gly as a sole organic sulfur source (Cys-Gly media), suggesting that, indeed, other enzymes could support Cys-Gly transport (Figure 2C). However, inactivation of NgtA had no impact on *F. novicida* growth in Cys-Gly media in either the wild-type or $\Delta dptA$ backgrounds. Together, these data suggest that NgtA is a transporter with specificity for intact GSH.

In the initial report of the Pht family of MFS transporters, the NgtA homolog of *F. tularensis* was the only member of its cluster.¹³ With many more genome sequences now available, we asked whether homologs of this protein could be found in other species. Using PSI-BLAST with the sequence of NgtA from *F. novicida* as the seed, we collected all publicly available sequences encoding MFS proteins from the Pht family and constructed a phylogeny. We found that although many of the clades in the phylogeny are dominated by sequences deriving from *Legionella* and *Coxiella* spp., the clade containing NgtA consists largely of sequences deriving from *Francisella* spp. and related *Thiotrichales*, with only two homologs found outside this group, in metagenome-assembled genomes of uncharacterized strains identified only as belonging to the Legionellales order and Coxiellaceae family, respectively (Figures 2D and 2E; Table S3). Our inability to identify NgtA orthologs more broadly suggests that this mechanism of transporting GSH may be an adaptation particularly exploited by organisms in this group.

A cytoplasmic GATase family enzyme that initiates GSH degradation

The finding that a GSH transporter can facilitate *F. novicida* growth in GSH media in the absence of Ggt and ChaC implies that this organism must encode cytoplasmic proteins capable of initiating GSH catabolism. The gene with the second strongest synthetic phenotype in our transposon mutant screen, FTN_0435, encodes a predicted GATase. Most GATase proteins function in biosynthetic reactions in which the amido group from glutamine is transferred to an acceptor substrate, generating glutamate and an aminated product.¹⁸ However, a limited

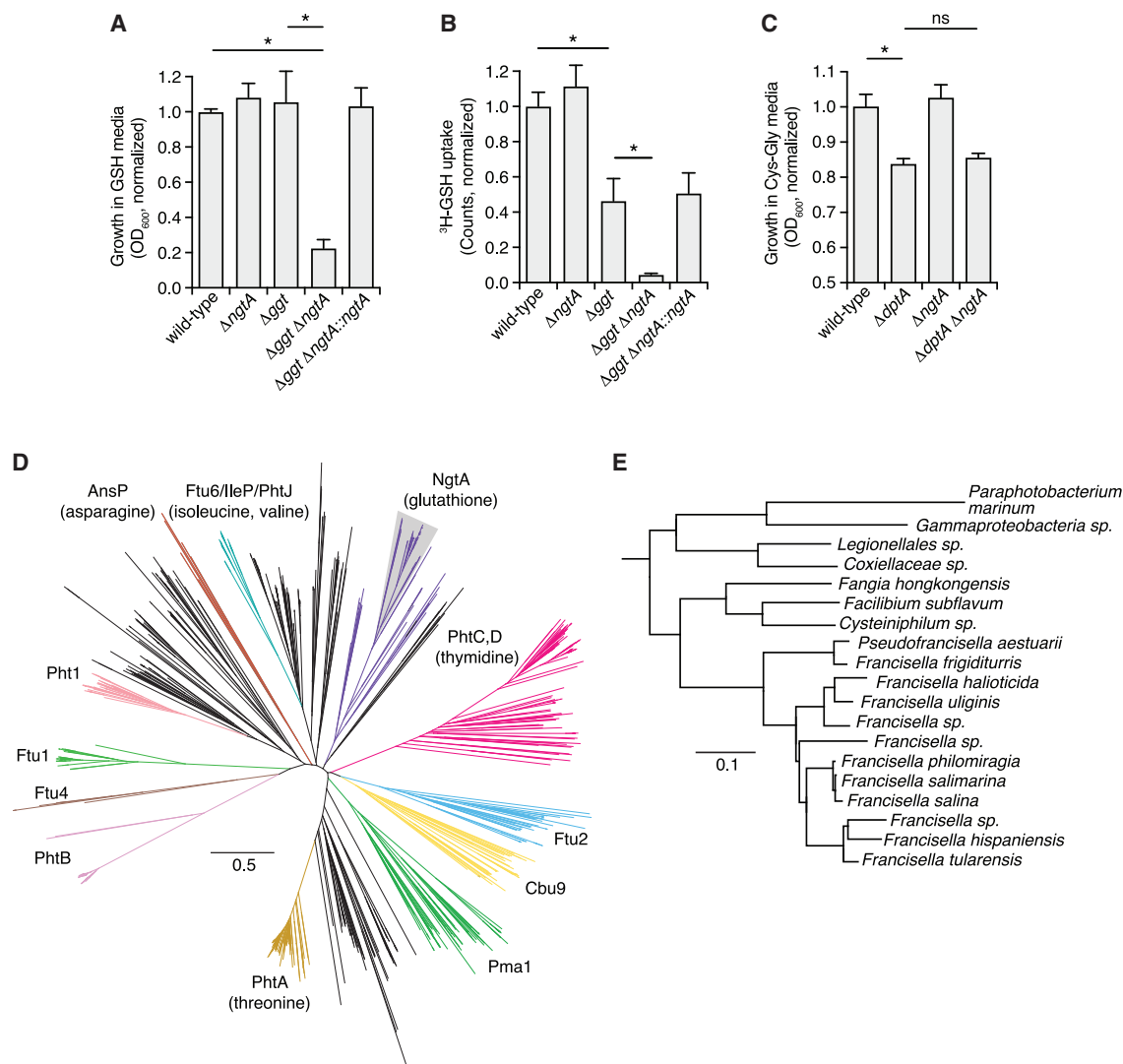


Figure 2. NgTA is a major facilitator superfamily protein that transports intact GSH in a Ggt-independent manner

(A) Normalized growth yields in GSH medium of the indicated *F. novicida* strains.

(B) Quantification of the level of [Glycine-2-³H]-Glutathione (³H-GSH) uptake in the indicated strains of *F. novicida* after 45 min incubation.

(C) Normalized growth yields of the indicated *F. novicida* strains after 36 h in defined medium containing Cys-Gly as a sole source of cysteine.

(D) Neighbor-joining phylogeny of proteins from the Pht family of MFS transporters. Colored clades contain sequences identified in the original description of the family or subsequently characterized.¹³ Representative proteins from the Chen et al. study or other reports are indicated by their respective clades, and transport substrates are indicated in parentheses when known. Candidate NgTA homologs are shown in purple, and the region of the phylogeny amplified in (E) is indicated (shading).

(E) Neighbor-joining phylogeny of NgTA homologs in *Francisella* and related genera. Species names indicate the source of the protein sequences. Data in (A)–(C) represent mean ± SD. Asterisks indicate statistically significant differences (unpaired two-tailed Student's *t* test; **p* < 0.05; ns, not significant). See also [Figure S2](#) and [Table S3](#).

number of GATase-domain-containing proteins instead function as catabolic enzymes that cleave γ -glutamyl bonds in assorted substrates, releasing glutamate. These include enzymes that hydrolyze such substrates as the folate storage and retention molecule poly(γ -glutamate), the spermidine degradation intermediate γ -glutamine- γ -aminobutyrate, GSH conjugates involved in glucosinolate synthesis and, notably, GSH itself.^{19–23} The latter was found to occur in yeast and is catalyzed by the enzyme Dug3p.²³

Structure modeling revealed that FTN_0435, herein named CgaA (cytosolic GSH amidotransferase A), shares an overall fold and a conserved predicted catalytic triad (C97, H184, E186) with class I GATases²⁴ (Figure 3A). This is in contrast to the GSH-targeting enzyme of yeast, a class II GATase.²³ Nevertheless, we found that, as predicted by our Tn-seq results, CgaA is required for *F. novicida* Δ ggt growth in GSH medium, a phenotype that could be genetically complemented (Figures 3B and 3C). Substitution of the predicted catalytic cysteine with alanine

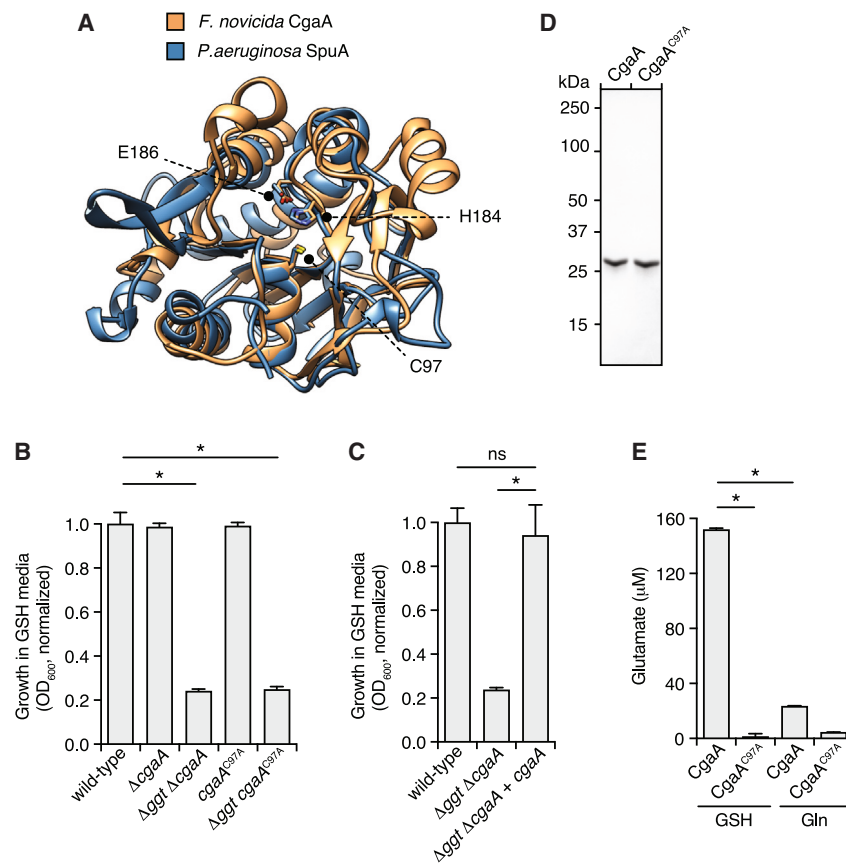


Figure 3. CgaA is a cytoplasmic glutamine amidotransferase (GATase) family protein that degrades GSH

(A) Alignment of the predicted structure of CgaA (orange) and the crystal structure of a characterized class I GATases, *P. aeruginosa* SpuA (blue, PDB: 7D4R, only one subunit of the SpuA homodimer is shown). The conserved catalytic triad is indicated (numbers correspond to amino acid positions in *F. novicida* CgaA).

(B and C) Normalized 36-h growth yields of the indicated strains of *F. novicida*.

(D) Coomassie-stained SDS-PAGE analysis of purified CgaA and CgaA^{C97A}.

(E) Glutamate released following 60-min incubation of purified CgaA or CgaA^{C97A} (1 μ M protein) with GSH or Gln (10 mM substrate). Data in (B), (C), and (E) represent means \pm SD. Asterisks represent statistically significant differences (unpaired two-tailed Student's *t* test; **p* < 0.05; ns, not significant). See also Figure S3.

(*cgaA*^{C97A}) had no impact on the protein level produced but recapitulated the growth phenotype of a *cgaA* deletion, supporting an enzymatic role for this protein in GSH catabolism (Figures 3B and S3A). We thus asked whether CgaA encodes a cytoplasmic enzyme able to initiate GSH degradation.

To determine the substrate specificity of CgaA, we used established *in vitro* assays to measure the activity of CgaA and CgaA^{C97A} purified from *E. coli*. Biosynthetic GATase proteins exhibit glutaminase activity, generating glutamate and ammonia in the absence of their respective amido-group-accepting substrates. However, we detected only a low level of glutamate accumulation following incubation of CgaA with glutamine. On the contrary, we readily detected glutamate released from GSH by CgaA, and this product was not detected above background levels in reactions with CgaA^{C97A} (Figures 3D and 3E). In total, these data support the hypothesis that CgaA is a GATase that acts downstream of NgT to initiate the degradation of GSH via cleavage into Glu and Cys-Gly.

Although our genetic and biochemical data strongly suggest that GSH is a physiological substrate of CgaA, we noted the rate of glutamate release from the purified enzyme is low. In yeast, the GATase enzyme Dug3p acts in concert with two other proteins, Dug1p and Dug2p.²³ Purified Dug3p is inactive *in vitro* unless bound to Dug2p, which allosterically activates the enzyme. Dug1p is a Cys-Gly-specific peptidase that does not physically associate with the Dug2p-Dug3p complex. CgaA is encoded by the third gene in a predicted five-gene operon. Examination of our Tn-seq results suggested that the genes en-

coded upstream of *cgaA* within this operon may also be important for growth on GSH in the *F. novicida* Δggt background (Figures S3B–S3D; Tables S1 and S2); however, we also considered that insertions within these genes may lead to polar effects on *cgaA*. To distinguish between these possibilities, we generated a conservative in-frame deletion in the first gene in the operon in *F. novicida* Δggt and measured the growth of this strain relative to *F. novicida* $\Delta ggt \Delta ngtA$ in GSH media. This strain exhibited robust growth in GSH media (Figure 3E), strongly suggesting that polar effects underlie the apparent depletion of genes upstream of *cgaA* in our Tn-seq study and, moreover, that CgaA does not require adjacently encoded proteins for its activity.

Parallel pathways for GSH catabolism contribute to *F. novicida* intramacrophage growth

Previous studies indicate that *ggt* mutants of *F. tularensis* SCHU S4 and LVS are attenuated in virulence.^{10,11,25–27} This has led to the consensus in the field that GSH serves as an important source of organic sulfur for these bacteria during infection.^{1,5,28} To our knowledge, the role of host GSH catabolism during *F. novicida* infection has not been examined. Unlike *F. tularensis* SCHU S4 and LVS, our results suggest that *F. novicida* may be capable of utilizing multiple pathways for GSH scavenging *in vivo*. To explore this possibility, we measured the growth of *F. novicida* strains lacking the function of one or both GSH uptake pathways in bone-marrow-derived murine macrophages (BMMs). Interestingly, we found that only *F. novicida* strains in which both pathways are inactivated display a detectable intracellular growth defect (Figure 4A). We next examined the importance of the two GSH catabolism pathways in a more complex model of infection, a murine intranasal model.²⁹ At 48 h post-infection in the intranasal model, we observed a modest decrease in recovery of *F. novicida* Δggt from lung samples. However, in contrast to our macrophage

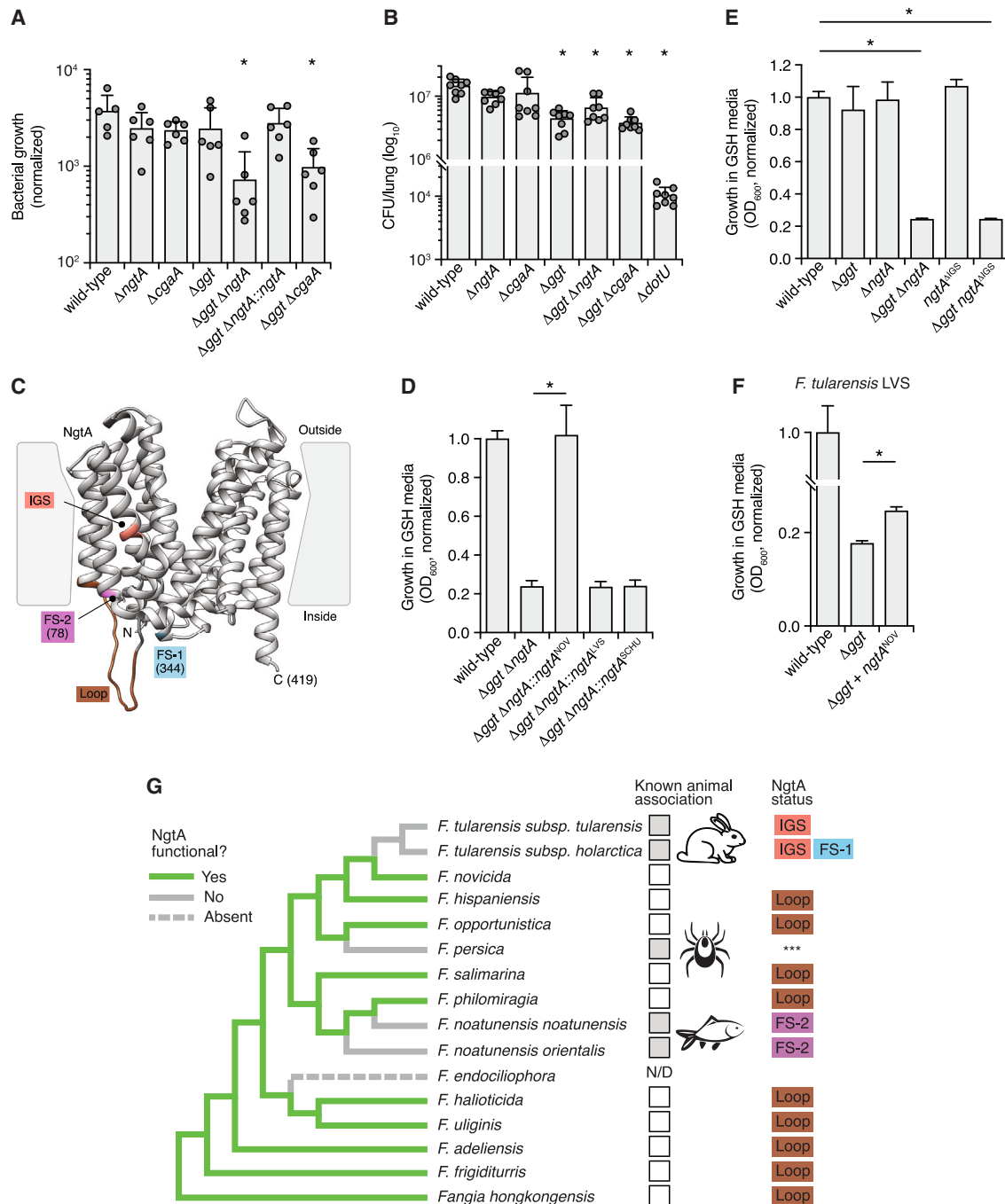


Figure 4. NgTA contributes to intramacrophage replication of *F. novicida* but is mutationally inactivated in pathogenic *Francisella* strains

(A) Normalized intracellular growth of the indicated strains of *F. novicida* in bone-marrow-derived murine macrophages (24 h post-infection).

(B) Bacterial burden in mouse lungs at 48 h post intranasal infection with ~100 colony-forming units (CFUs) of the indicated strains of *F. novicida*.

(C) Structural model of *F. novicida* NgTA, highlighting differences with NgTA in other *Francisella* species. The terminal residues resulting from truncating frameshift mutations (FS) indicated in parentheses. FS-1, location of truncation resulting from frameshift in *F. tularensis* subsp. *holarctica*; FS-2, location of truncation resulting from frameshift in *F. noatunensis*; loop, poorly conserved region with many differences between species; IGS, three-residue deletion found in *F. tularensis* subsp. *tularensis*. The first six and the last nine residues in the NgTA structure are trimmed.

(D–F) Normalized growth yields in GSH medium of the indicated strains of *F. novicida* (D) and (E) or *F. tularensis* LVS (F).

(G) Schematic phylogeny of *Francisella* species indicating predicted functionality of NgTA (functional, green; inactivated, solid gray; absent, dashed gray), animal association when known (mammal association indicated by rabbit schematic), and mutations present in *ngtA* (colors correspond to C). The *ngtA* sequence of *P. persica* contains many mutations (***), and *ngtA* appears to have been lost completely from *F. endocilliphora*. Phylogenetic relationships derived from Valles et al.³⁰ Data shown in (A), (B), and (D)–(F) represent means \pm SD. Data points in (A) and (B) indicate technical replicates from 3 (A) or 4 (B) biological replicates conducted. Asterisks indicate statistically significant differences (A) and (B), one-way ANOVA with Dunnett's multiple comparison test comparing mutant strains to wild type; (D–F, unpaired two-tailed Student's *t* test; **p* < 0.05; ns, not significant). See also [Figure S4](#).

infection study, no further decrease was detected when Δggt was combined with $\Delta ngtA$ or $\Delta cgaA$ (Figure 4B).

The results of our murine infection model study suggest that, in the context of an animal infection, Ggt-mediated cleavage of GSH may be the primary mechanism by which *F. novicida* acquires organic sulfur. This is consistent with the observation that *ggt* mutants of *F. tularensis* SCHU S4 and *F. tularensis* LVS have significant virulence defects; however, it remained unclear why *ggt* inactivation alone is sufficient to inhibit *in vitro* growth in GSH medium in these other subspecies, but not in *F. novicida*. Furthermore, the magnitude of virulence defect for the Δggt background of *F. novicida* is qualitatively lower than that of *F. tularensis* SCHU S4 and LVS.^{10,11,25–27} While investigating explanations for this difference, we found that the *ngtA* genes of SCHU S4 (*ngtA*^{SCHU}), LVS (*ngtA*^{LVS}), as well as those of other *F. tularensis* subsp. *tularensis* and subsp. *holarctica* strains encode proteins with a three-amino-acid deletion relative to *Ngta*^{NOV}. In the predicted structure of *Ngta*^{NOV}, these amino acids (I113-G114-S115) reside within a transmembrane helix located in the core of the protein (IGS, Figure 4C). *F. holarctica* *ngtA* genes further contain a small 5' in-frame deletion and a premature stop codon that removes the last two predicted transmembrane helices (FS-1, Figure 4C). Taken together with our current findings, these observations led us to hypothesize that *Ngta*, and thus GSH transport, is compromised in these pathogenic strains of *Francisella*. Indeed, we found that *F. novicida* Δggt carrying *ngtA*^{SCHU} or *ngtA*^{LVS} in place of *ngtA*^{NOV} demonstrated growth behavior matching *F. novicida* Δggt $\Delta ngtA$ in GSH medium (Figure 4D). Furthermore, *F. novicida* Δggt carrying *ngtA*^{NOV} engineered to contain only the three-residue deletion found in *ngtA* alleles from human pathogenic strains (*ngtA*^{IGS}) was similarly unable to grow in GSH medium (Figure 4E). All *Ngta* variants bearing Δ IGS were undetectable, despite efforts at enrichment by immunoprecipitation, suggesting that this deletion is sufficient to destabilize *Ngta* (Figure S4). We also performed the converse experiment in *F. tularensis* LVS by over-expressing *ngtA*^{NOV} in the Δggt background. The expression of *ngtA*^{NOV} resulted in a small, but reproducible restoration of growth in GSH medium (Figure 4F). We speculate that the limited degree to which *Ngta*^{NOV} expression restores *F. tularensis* LVS GSH autotrophy could be the result of pseudogenization or regulatory alteration of elements downstream of *Ngta* that are important for efficient GSH catabolism.

Our finding that *ngtA* is inactivated in multiple *F. tularensis* subspecies prompted us to examine the nature and prevalence of mutations in *ngtA* among *Francisella* spp. more broadly. Interestingly, we found evidence supporting pseudogenization of *ngtA* in two additional lineages of animal-associated *Francisella*: the tick endosymbiont *F. persica* and the fish pathogens *F. noatunensis* and *F. orientalis* (Figures 4C and 4G). On the contrary, the *ngtA* sequences of *Francisella* without a known animal association bore mutations primarily restricted to a hypervariable cytoplasmic loop that are not expected to inactivate the transporter (Figures 4C and 4G). Given that we find evidence for repeated *ngtA* pseudogenization events limited to *Francisella* lineages adapted to animal hosts, our results suggest that intact GSH uptake is most beneficial for bacteria in this genus in the environment, perhaps during replication within unicellular eukaryotes.

FupA is a porin that mediates GSH uptake

We were surprised to find *fupA* as a gene with highly differential transposon insertion frequency during growth on GSH versus cysteine as sole sulfur sources in both the wild-type and Δggt backgrounds of *F. novicida* (Figures 1B and 1C; Tables S1 and S2). *FupA* is a member of a family of paralogous predicted outer membrane proteins unique to *Francisella* species, several of which, including *FupA*, are widely thought to mediate high-affinity uptake of ferrous iron.^{31–33} Despite this dogma, *F. tularensis* SCHU S4 $\Delta fupA$ exhibits a general growth defect in minimal media regardless of iron source or type, and proteoliposome assays using purified *FupA* provide evidence that it promotes membrane permeability.^{31,34} We thus hypothesized that *FupA* may contribute to *F. novicida* growth in GSH media by facilitating GSH passage through the outer membrane.

To directly examine the role of *FupA* in GSH catabolism, we generated an in-frame deletion of *fupA* in the wild-type and Δggt backgrounds of *F. novicida*. Consistent with our Tn-seq results, deletion of *fupA* in both backgrounds resulted in a strong growth defect, specifically in GSH media (Figure 5A). We then evaluated the role of *FupA* in GSH transport by measuring the impact of $\Delta fupA$ on cellular uptake of ³H-GSH by *F. novicida*. We found that, in the absence of *FupA*, ³H-GSH uptake was reduced below levels observed in *F. novicida* Δggt (Figures 2B and 5B). Furthermore, inactivation of *ggt* in the $\Delta fupA$ background did not further reduce ³H-GSH uptake. These data support our hypothesis and further suggested that *FupA* could act as a general porin of *F. novicida*. Indeed, a prior analysis of predicted β -barrel proteins in *Francisella* did not identify clear homologs of previously characterized general porins.³⁵ In addition to serving as a conduit for the uptake of nutrients, a common feature of porins is that they present a vulnerability by providing entry to harmful molecules such as antibiotics and hydrogen peroxide.^{36,37} We found that *F. novicida* $\Delta fupA$ is significantly more resistant to hydrogen peroxide than the wild type, further supporting its functional assignment as a porin of *F. novicida* (Figure 5C). These findings show that GSH accesses the periplasm of *F. novicida* via *FupA*, thus providing an explanation for the insertion frequency in *fupA* observed in our screen. In total, our genetic, biochemical, and phenotypic data allow us to assemble a new, complete model for GSH transport and catabolism in *Francisella* (Figure 6).

DISCUSSION

In this study, we report the finding that *Francisella* spp. encode a previously uncharacterized, Ggt-independent pathway for GSH uptake that has been lost in each established animal-colonizing lineage of the genus. On one hand, the correlation between inactivation of the GSH transporter encoding gene *ngtA* and adaptation to animal association is counterintuitive, as GSH is only present at sufficient concentrations to be useful as a source of sulfur in host-associated environments. However, we found evidence that in *F. novicida*, a species without a known physiological animal host, *Ngta* and the intracellular GSH-degrading enzyme *CgaA* work in concert with *Ggt* to support intramacrophage replication. This was not observed in a mouse model of infection, where a range of cell types are infected.³⁸ The mechanisms macrophages employ to kill bacteria share many features in common

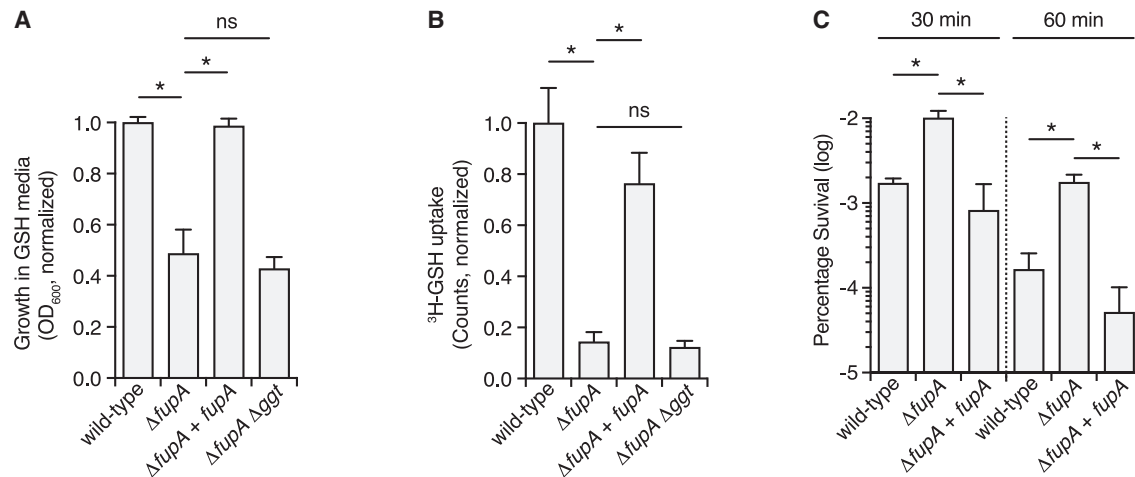


Figure 5. FupA is a porin required for GSH uptake in *F. novicida*

(A) Normalized growth in GSH medium of the indicated strains of *F. novicida*.

(B) Quantification of the level of ³H-GSH uptake in the indicated strains of *F. novicida* after 45 min incubation.

(C) Survival of the indicated strains of *F. novicida* after incubation of mid-log phase cultures with 1.5 mM H₂O₂ for 30 or 60 min. Data in (A)–(C) represent mean ± SD. Asterisks indicate statistically significant differences (unpaired two-tailed Student's t test; *p < 0.05; ns, not significant).

with those utilized by predatory protozoa.^{39–41} Although the environmental niches colonized by non-pathogenic *Francisella* species remain largely uncharacterized, several species have been isolated from bacterivorous ciliates, including the deeply branching species *F. adeliensis*, which encodes intact *ngtA*.^{30,42} Accordingly, we speculate that functional *NgTA* is maintained in environmental lineages due to its utility during colonization of a macrophage-like intracellular habitat within eukaryotic microbes. In support of an intracellular environment representing the natural niche of diverse *Francisella* species, species that encode functional *NgTA* also encode the host cell-targeting type VI secretion system associated with the *Francisella* pathogenicity island.^{43–45}

Unlike the GSH uptake mechanisms characterized in other bacterial pathogens, which consist of ABC transporters, intact GSH import in *Francisella* is mediated by an MFS transporter. The consequences of this are unclear; however, one difference between the transporter types is the steepness of the concentration gradient of GSH that each can overcome. ABC transporters rely on ATP and can achieve transport across gradients much steeper than those achievable with MFS transporters, which can only overcome concentration gradients equivalent to those of the coupling ions.⁴⁶ Interestingly, the bacteria in which ABC transporters for GSH have been identified, including *S. pneumoniae* and *H. influenzae*, reside in extracellular host-associated niches, where the concentration of GSH is much lower than the intracellular habitat of *F. novicida*.^{8,9,47} Thus, differences in the GSH concentration encountered in the different primary habitats these organisms colonize appears to correlate with the GSH uptake mechanism employed, in a manner consistent with the energetics of uptake by each route.

Although our data clearly demonstrate that *NgTA* is capable of transporting GSH and suggest it does not play a role in Cys-Gly import, we have not defined the extent of its physiologically relevant substrates. To our knowledge, the only other MFS protein previously shown to transport GSH is *Gex1* of yeast.⁴⁸ Although

Gex1 can export GSH, its primary function appears to be related to cadmium detoxification via the extrusion of GSH-cadmium conjugates. This raises the possibility that *NgTA* could transport substrates beyond GSH. Several other members of the Pht family of transporters to which *NgTA* belongs facilitate uptake of amino acids that are limiting during intracellular growth of *Francisella* and *Legionella*.^{15–17} Candidate additional substrates for *NgTA* could include other γ-Glu amide bonded molecules or a broader range of oligopeptides, such as those transported by members of the POT class of MFS proteins.⁴⁹

During both growth in GSH medium and intramacrophage replication, we find that either *Ggt* or *NgTA* and *CgaA*-mediated degradation of GSH are sufficient to support growth of *F. novicida*, raising the question as to why the two pathways are maintained in parallel in many strains. GSH plays several important roles beyond serving as a source of nutrients, including redox buffering, combating oxidative stress, and detoxifying metals and xenobiotics.⁵⁰ Import of intact GSH via *NgTA* could thus provide a source of GSH under conditions where *de novo* biosynthesis may provide an insufficient supply of the intact molecule to counteract particular stresses. For the non-pathogenic *Francisella* species in which we find intact *ngtA*, one such condition may be encountered during replication within a protozoan host. These organisms employ many of the same mechanisms for killing phagocytosed bacteria as macrophages, including generation of a reactive oxygen burst.⁴⁰ Interestingly, although *Francisella* have yet to be isolated from amoeba in a natural setting, laboratory studies employing model amoeba strains suggest that in these hosts, *Francisella* species replicate within the vacuole where the oxidative burst is delivered rather than escaping to the cytosol as in mammalian cell infections.^{51–54} Additionally, virulent strains of *Francisella* can limit the oxidative burst within cells they infect, by mechanisms that are not yet fully characterized^{55–57}; it remains to be determined whether these are conserved in other non-pathogenic species. We speculate that *NgTA* may provide a means of rapidly

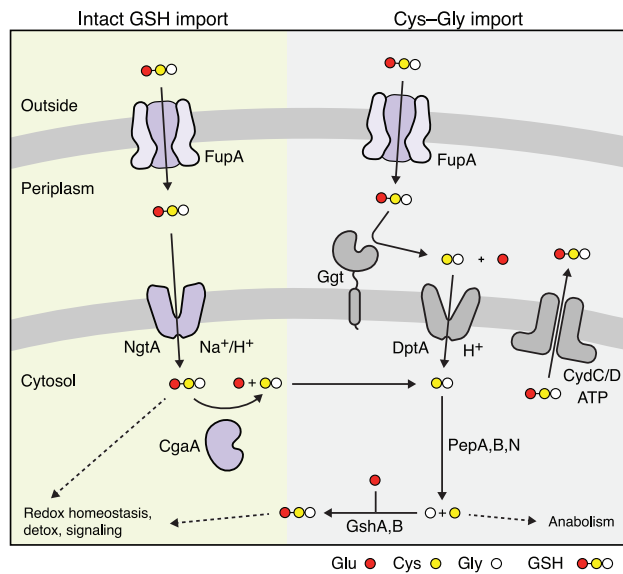


Figure 6. Comprehensive model of GSH transport and catabolism in *Francisella*

Both the pathways for import and cytosolic catabolism of GSH discovered in this study (left, green shading) and for periplasmic degradation of GSH and subsequent fate of imported Cys-Gly (right, gray shading) are indicated.

acquiring GSH for *Francisella* species that must contend with acute episodes of oxidative stress.

If the primary role of NgTA is to enable import of intact GSH for non-nutritional uses, the question then arises as to why *Francisella* species additionally encode an intracellular enzyme for GSH degradation, CgaA. In eukaryotic cells, constitutive degradation of GSH by intracellular enzymes contributes to GSH homeostasis. In yeast, this is mediated by the Dug complex, which shares the same predicted enzymatic function as CgaA, whereas in mammalian cells, constitutive turnover of GSH appears to be mediated by the γ -glutamyl cyclotransferase enzyme ChaC2.^{23,58,59} The ChaC2 homologs that have been characterized to date exhibit a very slow rate of GSH turnover, which has been suggested to be important for preventing unchecked depletion of intracellular GSH levels.⁵⁹ We similarly observed a low rate of GSH turnover by purified CgaA. Although this observed rate of turnover may be the result of our *in vitro* assay conditions, it is consistent with CgaA playing a role in GSH homeostasis. Of note, *Francisella* spp. also encode a homolog of ChaC2, but this protein localizes to the periplasm. Additionally, strains lacking ChaC exhibit pleiotropic phenotypes,¹¹ and the corresponding gene was not a strong hit in our Tn-seq screen for genes important in GSH utilization, suggesting its role in GSH catabolism is likely a minor part of its overall function in *Francisella*.

A previously missing component of the GSH utilization pathway in *Francisella* is the means by which the tripeptide crosses the outer membrane. Here, we provide evidence that FupA provides this function by acting as a porin. Our findings challenge the prior assertion that FupA serves as a high-affinity ferrous iron transporter.³³ Upon reexamination, two pieces of published data support our conclusion that FupA functions as a general porin: (1) unlike typical high-affinity transport mecha-

nisms, FupA expression is not induced by limiting iron, and (2) growth of *F. tularensis* $\Delta fupA$ is reduced in minimal media regardless of the concentration or type of iron supplied.^{31,33} Additionally, we note that in other Gram-negative species, porins related to OmpC or OmpF, which are absent in *Francisella* spp., allow passive entry of Fe^{2+} that is then imported across the inner membrane by high-affinity transporters.⁶⁰ Together with our discovery of the NgTA- and CgaA-mediated pathway for GSH uptake and degradation, our identification of the role of FupA in GSH import allows us to construct a substantially revised model for GSH catabolism in *Francisella* that highlights the central importance of this molecule for this diverse group of organisms.

STAR★METHODS

Detailed methods are provided in the online version of this paper and include the following:

- KEY RESOURCES TABLE
- RESOURCE AVAILABILITY
 - Lead contact
 - Materials availability
 - Data and code availability
- EXPERIMENTAL MODEL AND STUDY PARTICIPANT DETAILS
 - Bacterial strains and growth conditions
 - Murine bone marrow-derived macrophage generation
 - Mice
- METHOD DETAILS
 - Strain and plasmid construction
 - Transposon mutant library generation
 - Tn-seq screen
 - Tn-seq data processing
 - Bacterial growth assays
 - GSH uptake assays
 - Protein expression and purification
 - In vitro glutaminase assays
 - H₂O₂ sensitivity assays
 - Macrophage infection assays
 - *F. novicida* inoculum preparation and intranasal infection
 - Protein expression level analysis
 - NgTA sequence and phylogenetic analysis
- QUANTIFICATION AND STATISTICAL ANALYSIS

SUPPLEMENTAL INFORMATION

Supplemental information can be found online at <https://doi.org/10.1016/j.chom.2023.06.010>.

ACKNOWLEDGMENTS

The authors wish to thank members of the Mougous laboratory for helpful suggestions. This work was supported by the NIH (R01AI145954 to J.D.M., S.L.D., S.J. Skerrett, and J.C.; P30 DK089507 to S.J. Salipante), the Defense Advanced Research Projects Agency Biological Technologies Office Program: Harnessing Enzymatic Activity for Lifesaving Remedies (HEALR) under cooperative agreement no. HR0011-21-2-0012 (to J.D.M. and J.J.W.), and the Cystic Fibrosis Foundation (SINGH19R0 to St.J.S.). J.D.M. is an HHMI Investigator and is supported by the Lynn M. and Michael D. Garvey Endowed Chair at the University of Washington.

AUTHOR CONTRIBUTIONS

Y.W., H.E.L., S.B.P., and J.D.M. conceived the study. Y.W., H.E.L., L.S.M.K., S.B.P., J.C., and J.D.M. designed the study. Y.W., H.E.L., C.A.T., S.K., E.L., J.C.C., L.S.M.K., Q.T., Q.C., G.F.R., and K.M.P. performed experiments. Y.W., H.E.L., L.A.G., M.C.R., Y.L., and S.B.P. processed, analyzed, and visualized the data. Y.W., S.B.P., and J.D.M. wrote the manuscript. S.T., S.J. Skerrett, S.J. Salipante, N.S.B., J.J.W., S.L.D., S.B.P., J.C., and J.D.M. provided supervision. S.J. Skerrett, S.J. Salipante, J.J.W., S.L.D., J.C., and J.D.M. provided funding. All authors contributed to manuscript editing and support the conclusions.

DECLARATION OF INTERESTS

The authors declare no competing interests.

Received: January 25, 2023

Revised: May 19, 2023

Accepted: June 20, 2023

Published: July 14, 2023

REFERENCES

1. Abu Kwaik, Y., and Bumann, D. (2013). Microbial quest for food in vivo: 'nutritional virulence' as an emerging paradigm. *Cell. Microbiol.* *15*, 882–890. <https://doi.org/10.1111/cmi.12138>.
2. Niu, H., Xiong, Q., Yamamoto, A., Hayashi-Nishino, M., and Rikihisa, Y. (2012). Autophagosomes induced by a bacterial Beclin 1 binding protein facilitate obligatory intracellular infection. *Proc. Natl. Acad. Sci. USA* *109*, 20800–20807. <https://doi.org/10.1073/pnas.1218674109>.
3. Price, C.T., Al-Quadani, T., Santic, M., Rosenshine, I., and Abu Kwaik, Y. (2011). Host proteasomal degradation generates amino acids essential for intracellular bacterial growth. *Science* *334*, 1553–1557. <https://doi.org/10.1126/science.1212868>.
4. Meister, A., and Anderson, M.E. (1983). Glutathione. *Annu. Rev. Biochem.* *52*, 711–760. <https://doi.org/10.1146/annurev.bi.52.070183.003431>.
5. Ku, J.W., and Gan, Y.H. (2019). Modulation of bacterial virulence and fitness by host glutathione. *Curr. Opin. Microbiol.* *47*, 8–13. <https://doi.org/10.1016/j.mib.2018.10.004>.
6. Reniere, M.L., Whiteley, A.T., Hamilton, K.L., John, S.M., Lauer, P., Brennan, R.G., and Portnoy, D.A. (2015). Glutathione activates virulence gene expression of an intracellular pathogen. *Nature* *517*, 170–173. <https://doi.org/10.1038/nature14029>.
7. Wong, J., Chen, Y., and Gan, Y.H. (2015). Host Cytosolic Glutathione Sensing by a Membrane Histidine Kinase Activates the Type VI Secretion System in an Intracellular Bacterium. *Cell Host Microbe* *18*, 38–48. <https://doi.org/10.1016/j.chom.2015.06.002>.
8. Potter, A.J., Trappetti, C., and Paton, J.C. (2012). *Streptococcus pneumoniae* uses glutathione to defend against oxidative stress and metal ion toxicity. *J. Bacteriol.* *194*, 6248–6254. <https://doi.org/10.1128/JB.01393-12>.
9. Vergauwen, B., Elegheert, J., Dansercoer, A., Devreese, B., and Savvides, S.N. (2010). Glutathione import in *Haemophilus influenzae* Rd is primed by the periplasmic heme-binding protein HbpA. *Proc. Natl. Acad. Sci. USA* *107*, 13270–13275. <https://doi.org/10.1073/pnas.1005198107>.
10. Alkhuder, K., Meibom, K.L., Dubail, I., Dupuis, M., and Charbit, A. (2009). Glutathione provides a source of cysteine essential for intracellular multiplication of *Francisella tularensis*. *PLoS Pathog.* *5*, e1000284. <https://doi.org/10.1371/journal.ppat.1000284>.
11. Ramsey, K.M., Ledvina, H.E., Tresko, T.M., Wandzilak, J.M., Tower, C.A., Tallo, T., Schramm, C.E., Peterson, S.B., Skerrett, S.J., Mougous, J.D., and Dove, S.L. (2020). TN-Seq reveals hidden complexity in the utilization of host-derived glutathione in *Francisella tularensis*. *PLoS Pathog.* *16*, e1008566. <https://doi.org/10.1371/journal.ppat.1008566>.
12. Drew, D., North, R.A., Nagarathinam, K., and Tanabe, M. (2021). Structures and general transport mechanisms by the major facilitator superfamily (MFS). *Chem. Rev.* *121*, 5289–5335. <https://doi.org/10.1021/acs.chemrev.0c00983>.
13. Chen, D.E., Podell, S., Sauer, J.D., Swanson, M.S., and Saier, M.H. (2008). The phagosomal nutrient transporter (Pht) family. *Microbiology (Reading)* *154*, 42–53. <https://doi.org/10.1099/mic.0.2007/010611-0>.
14. Fonseca, M.V., Sauer, J.D., Crepin, S., Byrne, B., and Swanson, M.S. (2014). The phtC-phtD locus equips *Legionella pneumophila* for thymidine salvage and replication in macrophages. *Infect. Immun.* *82*, 720–730. <https://doi.org/10.1128/IAI.01043-13>.
15. Gesbert, G., Ramond, E., Rigard, M., Frapy, E., Dupuis, M., Dubail, I., Barel, M., Henry, T., Meibom, K., and Charbit, A. (2014). Asparagine assimilation is critical for intracellular replication and dissemination of *Francisella*. *Cell. Microbiol.* *16*, 434–449. <https://doi.org/10.1111/cmi.12227>.
16. Gesbert, G., Ramond, E., Tros, F., Dairou, J., Frapy, E., Barel, M., and Charbit, A. (2015). Importance of branched-chain amino acid utilization in *Francisella* intracellular adaptation. *Infect. Immun.* *83*, 173–183. <https://doi.org/10.1128/IAI.02579-14>.
17. Sauer, J.D., Bachman, M.A., and Swanson, M.S. (2005). The phagosomal transporter A couples threonine acquisition to differentiation and replication of *Legionella pneumophila* in macrophages. *Proc. Natl. Acad. Sci. USA* *102*, 9924–9929. <https://doi.org/10.1073/pnas.0502767102>.
18. Massière, F., and Badet-Denisot, M.A. (1998). The mechanism of glutamine-dependent amidotransferases. *Cell. Mol. Life Sci.* *54*, 205–222. <https://doi.org/10.1007/s000180050145>.
19. Chen, Y., Jia, H., Zhang, J., Liang, Y., Liu, R., Zhang, Q., and Bartlam, M. (2021). Structure and mechanism of the gamma-glutamyl-gamma-aminobutyrate hydrolase SpuA from *Pseudomonas aeruginosa*. *Acta Crystallogr. D Struct. Biol.* *77*, 1305–1316. <https://doi.org/10.1107/S2059798321008986>.
20. Geu-Flores, F., Møldrup, M.E., Böttcher, C., Olsen, C.E., Scheel, D., and Halkier, B.A. (2011). Cytosolic gamma-glutamyl peptidases process glutathione conjugates in the biosynthesis of glucosinolates and camalexin in *Arabidopsis*. *Plant Cell* *23*, 2456–2469. <https://doi.org/10.1105/tpc.111.083998>.
21. Kurihara, S., Oda, S., Kumagai, H., and Suzuki, H. (2006). Gamma-glutamyl-gamma-aminobutyrate hydrolase in the putrescine utilization pathway of *Escherichia coli* K-12. *FEMS Microbiol. Lett.* *256*, 318–323. <https://doi.org/10.1111/j.1574-6968.2006.00137.x>.
22. Li, H., Ryan, T.J., Chave, K.J., and Van Roey, P. (2002). Three-dimensional structure of human gamma-glutamyl hydrolase. A class I glutamine amidotransferase adapted for a complex substrate. *J. Biol. Chem.* *277*, 24522–24529. <https://doi.org/10.1074/jbc.M202020200>.
23. Kaur, H., Ganguli, D., and Bachhawat, A.K. (2012). Glutathione degradation by the alternative pathway (DUG pathway) in *Saccharomyces cerevisiae* is initiated by (Dug2p-Dug3p)2 complex, a novel glutamine amidotransferase (GATase) enzyme acting on glutathione. *J. Biol. Chem.* *287*, 8920–8931. <https://doi.org/10.1074/jbc.M111.327411>.
24. Moulleron, S., and Golinelli-Pimpaneau, B. (2007). Conformational changes in ammonia-channeling glutamine amidotransferases. *Curr. Opin. Struct. Biol.* *17*, 653–664. <https://doi.org/10.1016/j.sbi.2007.09.003>.
25. Ireland, P.M., LeButt, H., Thomas, R.M., and Oyston, P.C.F. (2011). A *Francisella tularensis* SCHU S4 mutant deficient in gamma-glutamyltransferase activity induces protective immunity: characterization of an attenuated vaccine candidate. *Microbiology (Reading)* *157*, 3172–3179. <https://doi.org/10.1099/mic.0.052902-0>.
26. Kadzhaev, K., Zingmark, C., Golovliv, I., Bolanowski, M., Shen, H., Conlan, W., and Sjöstedt, A. (2009). Identification of genes contributing to the virulence of *Francisella tularensis* SCHU S4 in a mouse intradermal infection model. *PLoS One* *4*, e5463. <https://doi.org/10.1371/journal.pone.0005463>.
27. Qin, A., and Mann, B.J. (2006). Identification of transposon insertion mutants of *Francisella tularensis* tularensis strain Schu S4 deficient in intracellular replication in the hepatic cell line HepG2. *BMC Microbiol.* *6*, 69. <https://doi.org/10.1186/1471-2180-6-69>.

28. Meibom, K.L., and Charbit, A. (2010). *Francisella tularensis* metabolism and its relation to virulence. *Front. Microbiol.* *1*, 140. <https://doi.org/10.3389/fmicb.2010.00140>.
29. Lauriano, C.M., Barker, J.R., Yoon, S.S., Nano, F.E., Arulanandam, B.P., Hassett, D.J., and Kloos, K.E. (2004). MglA regulates transcription of virulence factors necessary for *Francisella tularensis* intraamoebae and intramacrophage survival. *Proc. Natl. Acad. Sci. USA* *101*, 4246–4249. <https://doi.org/10.1073/pnas.0307690101>.
30. Vallesi, A., Sjödin, A., Petrelli, D., Luporini, P., Taddei, A.R., Thelau, J., Öhrman, C., Nilsson, E., Di Giuseppe, G., Gutiérrez, G., and Villalobo, E. (2019). A new species of the gamma-proteobacterium *Francisella*, *F. adeliensis* Sp. Nov., Endocytobiont in an Antarctic marine ciliate and potential evolutionary forerunner of pathogenic species. *Microb. Ecol.* *77*, 587–596. <https://doi.org/10.1007/s00248-018-1256-3>.
31. Lindgren, H., Honn, M., Golovlev, I., Kadzhaev, K., Conlan, W., and Sjöstedt, A. (2009). The 58-kilodalton major virulence factor of *Francisella tularensis* is required for efficient utilization of iron. *Infect. Immun.* *77*, 4429–4436. <https://doi.org/10.1128/IAI.00702-09>.
32. Ramakrishnan, G., and Sen, B. (2014). The FupA/B protein uniquely facilitates transport of ferrous iron and siderophore-associated ferric iron across the outer membrane of *Francisella tularensis* live vaccine strain. *Microbiology (Reading)* *160*, 446–457. <https://doi.org/10.1099/mic.0.072835-0>.
33. Ramakrishnan, G., Sen, B., and Johnson, R. (2012). Paralogous outer membrane proteins mediate uptake of different forms of iron and synergistically govern virulence in *Francisella tularensis*. *J. Biol. Chem.* *287*, 25191–25202. <https://doi.org/10.1074/jbc.M112.371856>.
34. Siebert, C., Mercier, C., Martin, D.K., Renesto, P., and Schaack, B. (2020). Physicochemical evidence that *Francisella* FupA and FupB proteins are porins. *Int. J. Mol. Sci.* *21*, 5496. <https://doi.org/10.3390/ijms21155496>.
35. Huntley, J.F., Conley, P.G., Hagman, K.E., and Norgard, M.V. (2007). Characterization of *Francisella tularensis* outer membrane proteins. *J. Bacteriol.* *189*, 561–574. <https://doi.org/10.1128/JB.01505-06>.
36. Delcour, A.H. (2009). Outer membrane permeability and antibiotic resistance. *Biochim. Biophys. Acta* *1794*, 808–816. <https://doi.org/10.1016/j.bbapap.2008.11.005>.
37. van der Heijden, J., Reynolds, L.A., Deng, W., Mills, A., Scholz, R., Imami, K., Foster, L.J., Duong, F., and Finlay, B.B. (2016). *Salmonella* rapidly regulates membrane permeability to survive oxidative stress. *mBio* *7*, e01238–e01216. <https://doi.org/10.1128/mBio.01238-16>.
38. Hall, J.D., Woolard, M.D., Gunn, B.M., Craven, R.R., Taft-Benz, S., Frelinger, J.A., and Kawula, T.H. (2008). Infected-host-cell repertoire and cellular response in the lung following inhalation of *Francisella tularensis* Schu S4, LVS, or U112. *Infect. Immun.* *76*, 5843–5852. <https://doi.org/10.1128/IAI.01176-08>.
39. German, N., Doyscher, D., and Rensing, C. (2013). Bacterial killing in macrophages and amoeba: do they all use a brass dagger? *Future Microbiol.* *8*, 1257–1264. <https://doi.org/10.2217/fmb.13.100>.
40. Siddiqui, R., and Khan, N.A. (2012). *Acanthamoeba* is an evolutionary ancestor of macrophages: a myth or reality? *Exp. Parasitol.* *130*, 95–97. <https://doi.org/10.1016/j.exppara.2011.11.005>.
41. Sun, S., Noorian, P., and McDougald, D. (2018). Dual role of mechanisms involved in resistance to predation by protozoa and virulence to humans. *Front. Microbiol.* *9*, 1017. <https://doi.org/10.3389/fmicb.2018.01017>.
42. Sjödin, A., Öhrman, C., Bäckman, S., Lärkeryd, A., Granberg, M., Lundmark, E., Karlsson, E., Nilsson, E., Vallesi, A., Tellgren-Roth, C., et al. (2014). Complete Genome Sequence of *Francisella endociliophora* Strain FSC1006, Isolated from a Laboratory Culture of the Marine Ciliate *euplotes raikovi*. *Genome Announc.* *2*, e01227–e01214. <https://doi.org/10.1128/genomeA.01227-14>.
43. Challacombe, J.F., Petersen, J.M., Gallegos-Graves, V., Hodge, D., Pillai, S., and Kuske, C.R. (2017). Whole-genome relationships among *Francisella* bacteria of diverse origins define new species and provide specific regions for detection. *Appl. Environ. Microbiol.* *83*, e02589–e02516. <https://doi.org/10.1128/AEM.02589-16>.
44. Eshraghi, A., Kim, J., Walls, A.C., Ledvina, H.E., Miller, C.N., Ramsey, K.M., Whitney, J.C., Radey, M.C., Peterson, S.B., Ruhland, B.R., et al. (2016). Secreted effectors encoded within and outside of the *Francisella* Pathogenicity Island promote intramacrophage growth. *Cell Host Microbe* *20*, 573–583. <https://doi.org/10.1016/j.chom.2016.10.008>.
45. Kumar, R., Bröms, J.E., and Sjöstedt, A. (2020). Exploring the diversity within the genus *Francisella* - an integrated pan-genome and genome-mining approach. *Front. Microbiol.* *11*, 1928. <https://doi.org/10.3389/fmicb.2020.01928>.
46. Zhang, X.C., Han, L., and Zhao, Y. (2016). Thermodynamics of ABC transporters. *Protein Cell* *7*, 17–27. <https://doi.org/10.1007/s13238-015-0211-z>.
47. Smith, C.V., Jones, D.P., Guenther, T.M., Lash, L.H., and Lauterburg, B.H. (1996). Compartmentation of glutathione: implications for the study of toxicity and disease. *Toxicol. Appl. Pharmacol.* *140*, 1–12. <https://doi.org/10.1006/taap.1996.0191>.
48. Dhaoui, M., Auchère, F., Blaiseau, P.L., Lesuisse, E., Landoulsi, A., Camadro, J.M., Haguenaer-Tsapis, R., and Belgareh-Touzé, N. (2011). Gex1 is a yeast glutathione exchanger that interferes with pH and redox homeostasis. *Mol. Biol. Cell* *22*, 2054–2067. <https://doi.org/10.1091/mbc.E10-11-0906>.
49. Martínez Molledo, M., Quistgaard, E.M., Flayhan, A., Pieprzyk, J., and Löw, C. (2018). Multispecific substrate recognition in a proton-dependent oligopeptide transporter. *Structure* *26*, 467–476.e4. <https://doi.org/10.1016/j.str.2018.01.005>.
50. Pompella, A., Visvikis, A., Paolicchi, A., De Tata, V., and Casini, A.F. (2003). The changing faces of glutathione, a cellular protagonist. *Biochem. Pharmacol.* *66*, 1499–1503. [https://doi.org/10.1016/s0006-2952\(03\)00504-5](https://doi.org/10.1016/s0006-2952(03)00504-5).
51. Abd, H., Johansson, T., Golovliov, I., Sandström, G., and Forsman, M. (2003). Survival and growth of *Francisella tularensis* in *Acanthamoeba castellanii*. *Appl. Environ. Microbiol.* *69*, 600–606. <https://doi.org/10.1128/AEM.69.1.600-606.2003>.
52. El-Etr, S.H., Margolis, J.J., Monack, D., Robison, R.A., Cohen, M., Moore, E., and Rasley, A. (2009). *Francisella tularensis* type A strains cause the rapid encystment of *Acanthamoeba castellanii* and survive in amoebal cysts for three weeks postinfection. *Appl. Environ. Microbiol.* *75*, 7488–7500. <https://doi.org/10.1128/AEM.01829-09>.
53. Santic, M., Ozanic, M., Semic, V., Pavokovic, G., Mrcvic, V., and Kwaik, Y.A. (2011). Intra-vacuolar proliferation of *F. novicida* within *H. Vermiformis*. *Front. Microbiol.* *2*, 78. <https://doi.org/10.3389/fmicb.2011.00078>.
54. Ozanic, M., Marecic, V., Abu Kwaik, Y., and Santic, M. (2015). The divergent intracellular lifestyle of *Francisella tularensis* in evolutionarily distinct Host Cells. *PLoS Pathog.* *11*, e1005208. <https://doi.org/10.1371/journal.ppat.1005208>.
55. Child, R., Wehrly, T.D., Rockx-Brouwer, D., Dorward, D.W., and Celli, J. (2010). Acid phosphatases do not contribute to the pathogenesis of type A *Francisella tularensis*. *Infect. Immun.* *78*, 59–67. <https://doi.org/10.1128/IAI.00965-09>.
56. McCaffrey, R.L., and Allen, L.A. (2006). *Francisella tularensis* LVS evades killing by human neutrophils via inhibition of the respiratory burst and phagosome escape. *J. Leukoc. Biol.* *80*, 1224–1230. <https://doi.org/10.1189/jlb.0406287>.
57. Mohapatra, N.P., Soni, S., Rajaram, M.V., Dang, P.M., Reilly, T.J., El-Benna, J., Clay, C.D., Schlesinger, L.S., and Gunn, J.S. (2010). *Francisella* acid phosphatases inactivate the NADPH oxidase in human phagocytes. *J. Immunol.* *184*, 5141–5150. <https://doi.org/10.4049/jimmunol.0903413>.
58. Baudouin-Cornu, P., Lagniel, G., Kumar, C., Huang, M.E., and Labarre, J. (2012). Glutathione degradation is a key determinant of glutathione homeostasis. *J. Biol. Chem.* *287*, 4552–4561. <https://doi.org/10.1074/jbc.M111.315705>.
59. Kaur, A., Gautam, R., Srivastava, R., Chandel, A., Kumar, A., Karthikeyan, S., and Bachhawat, A.K. (2017). ChaC2, an enzyme for slow turnover of

- cytosolic glutathione. *J. Biol. Chem.* 292, 638–651. <https://doi.org/10.1074/jbc.M116.727479>.
60. Gerken, H., Vuong, P., Soparkar, K., and Misra, R. (2020). Roles of the EnvZ/OmpR two-component system and porins in iron acquisition in *Escherichia coli*. *mBio* 11. e01192-e01120. <https://doi.org/10.1128/mBio.01192-20>.
61. LoVullo, E.D., Molins-Schneekloth, C.R., Schweizer, H.P., and Pavelka, M.S., Jr. (2009). Single-copy chromosomal integration systems for *Francisella tularensis*. *Microbiology (Reading)* 155, 1152–1163. <https://doi.org/10.1099/mic.0.022491-0>.
62. Charity, J.C., Costante-Hamm, M.M., Balon, E.L., Boyd, D.H., Rubin, E.J., and Dove, S.L. (2007). Twin RNA polymerase-associated proteins control virulence gene expression in *Francisella tularensis*. *PLoS Pathog.* 3, e84.
63. Ledvina, H.E., Kelly, K.A., Eshraghi, A., Plemel, R.L., Peterson, S.B., Lee, B., Steele, S., Adler, M., Kawula, T.H., Merz, A.J., et al. (2018). A phosphatidylinositol 3-kinase effector alters phagosomal maturation to promote intracellular growth of *Francisella*. *Cell Host Microbe* 24, 285–295.e8. <https://doi.org/10.1016/j.chom.2018.07.003>.
64. Chamberlain, R.E. (1965). Evaluation of live tularemia vaccine prepared in a chemically defined medium. *Appl. Microbiol.* 13, 232–235.
65. Zaide, G., Grosfeld, H., Ehrlich, S., Zvi, A., Cohen, O., and Shafferman, A. (2011). Identification and characterization of novel and potent transcription promoters of *Francisella tularensis*. *Appl. Environ. Microbiol.* 77, 1608–1618. <https://doi.org/10.1128/AEM.01862-10>.
66. Maier, T.M., Havig, A., Casey, M., Nano, F.E., Frank, D.W., and Zahrt, T.C. (2004). Construction and characterization of a highly efficient *Francisella* shuttle plasmid. *Appl. Environ. Microbiol.* 70, 7511–7519. <https://doi.org/10.1128/AEM.70.12.7511-7519.2004>.
67. Gallagher, L.A. (2019). Methods for Tn-seq analysis in *Acinetobacter baumannii*. *Methods Mol. Biol.* 1946, 115–134. https://doi.org/10.1007/978-1-4939-9118-1_12.
68. Gallagher, L.A., Bailey, J., and Manoil, C. (2020). Ranking essential bacterial processes by speed of mutant death. *Proc. Natl. Acad. Sci. USA* 117, 18010–18017. <https://doi.org/10.1073/pnas.2001507117>.
69. Laemmli, U.K. (1970). Cleavage of structural proteins during the assembly of the head of bacteriophage T4. *Nature* 227, 680–685. <https://doi.org/10.1038/227680a0>.

STAR★METHODS

KEY RESOURCES TABLE

REAGENT or RESOURCE	SOURCE	IDENTIFIER
Antibodies		
Rabbit polyclonal anti-VSV-G	Sigma-Aldrich	Cat#V4888; RRID:AB_261872
Rabbit polyclonal anti-FLAG	Sigma-Aldrich	Cat#F7425; RRID:AB_439687
Rabbit anti-SodB	Gift from Dr. Karsten Hazlett	N/A
Goat anti-Rabbit HRP conjugated	Sigma-Aldrich	Cat#A6154; RRID:AB_258284
Anti-FLAG affinity resin	Thermo Scientific	Cat#A36803
Bacterial and virus strains		
<i>Francisella novicida</i> U112	Gift from Dr. Colin Manoil	N/A
<i>F. novicida</i> Δ ggt	Ramsey et al. ¹¹	N/A
<i>F. novicida</i> Δ chaC	Ramsey et al. ¹¹	N/A
<i>F. novicida</i> Δ ngtA	This paper	N/A
<i>F. novicida</i> Δ ggt Δ ngtA	This paper	N/A
<i>F. novicida</i> Δ ggt Δ ngtA::ngtA	This paper	N/A
<i>F. novicida</i> Δ dptA	This paper	N/A
<i>F. novicida</i> Δ dptA Δ ngtA	This paper	N/A
<i>F. novicida</i> Δ ggt Δ chaC	Ramsey et al. ¹¹	N/A
<i>F. novicida</i> Δ ggt Δ chaC Δ ngtA	This paper	N/A
<i>F. novicida</i> Δ cgaA	This paper	N/A
<i>F. novicida</i> Δ ggt Δ cgaA	This paper	N/A
<i>F. novicida</i> cgaA ^{C97A}	This paper	N/A
<i>F. novicida</i> Δ ggt cgaA ^{C97A}	This paper	N/A
<i>F. novicida</i> Δ ggt Δ cgaA + Tn7:Pnat-cgaA	This paper	N/A
<i>F. novicida</i> Δ ggt cgaA-VSV-G	This paper	N/A
<i>F. novicida</i> Δ ggt cgaA ^{C97A} -VSV-G	This paper	N/A
<i>F. novicida</i> Δ ggt Δ FTN_0433	This paper	N/A
<i>F. novicida</i> Δ dotU	Eshraghi et al. ⁴⁴	N/A
<i>F. novicida</i> Δ ggt Δ ngtA::ngtA ^{LVS}	This paper	N/A
<i>F. novicida</i> Δ ggt Δ ngtA::ngtA ^{SCHU}	This paper	N/A
<i>F. novicida</i> ngtA ^{ΔIGS}	This paper	N/A
<i>F. novicida</i> Δ ggt ngtA ^{ΔIGS}	This paper	N/A
<i>F. novicida</i> Δ ggt ngtA-3xFLAG	This paper	N/A
<i>F. novicida</i> Δ ggt ngtA ^{ΔIGS} -3xFLAG	This paper	N/A
<i>F. novicida</i> Δ ggt Δ ngtA::ngtA ^{SCHU} -3xFLAG	This paper	N/A
<i>F. novicida</i> Δ ggt Δ ngtA::ngtA ^{LVS} -3xFLAG	This paper	N/A
<i>F. novicida</i> Δ fupA	This paper	N/A
<i>F. novicida</i> Δ fupA + Tn7:Pbfr-fupA	This paper	N/A
<i>F. novicida</i> Δ fupA Δ ggt	This paper	N/A
<i>F. novicida</i> MFN245	Gift from Dr. Colin Manoil	N/A
<i>F. novicida</i> MFN245 Tn7:Pbfr-fupA	This paper	N/A
<i>F. tularensis</i> LVS	Gift from Dr. Karen Elkins	N/A
<i>F. tularensis</i> LVS Δ ggt	Ramsey et al. ¹¹	N/A
<i>Escherichia coli</i> DH5 α	Thermo Fisher Scientific	Cat#18258012
<i>E. coli</i> BL21 (DE3)	EMD Millipore	Cat#69450
Chemicals, peptides, and recombinant proteins		
[Glycine-2- ³ H]-Glutathione	PerkinElmer	Cat#NET282050UC

(Continued on next page)

Continued

REAGENT or RESOURCE	SOURCE	IDENTIFIER
Ecoscint Ultra	National Diagnostics	Cat# LS-270
Hydrogen peroxide solution	Sigma	Cat#H1009-5ML
Dulbecco's Modified Eagle's Medium	Corning	Cat#10-014-CM
Fetal Bovine Serum	Atlanta Biologicals	Cat#S10350H
L-929 mouse-fibroblast conditioned medium	This paper	N/A
Phosphate buffered saline	Corning	Cat#21-030-CV
Cation-free PBS	Corning	Cat#21-040-CV
Phosphate buffered saline	Life Technologies	Cat#10010049
Sodium deoxycholate	Sigma	Cat#D6750
IGEPAL	MP Biomedicals	Cat#198596
Critical commercial assays		
Glutamate Assay Kit	Abcam	Cat#ab83389
DNeasy Blood & Tissue Kit	Qiagen	Cat#69506
Deposited data		
Transposon insertion sequencing data	This paper	NCBI Sequence Read Archive: PRJNA967744
Experimental models: Organisms/strains		
C57BL/6J mice	The Jackson Laboratory	Cat#000664
Murine bone marrow-derived macrophages (BMMs) differentiated from bone marrow of female, 6-12 -weeks-old C57BL/6J mice	The Jackson Laboratory	Cat#000664
Oligonucleotides		
Primers are listed in Table S4	N/A	N/A
Recombinant DNA		
pEX18-pheS-km	Eshraghi et al. ⁴⁴	N/A
pEX18-pheS-km- <i>Δ</i> ggf	Ramsey et al. ¹¹	N/A
pEX18-pheS-km- <i>Δ</i> chaC	Ramsey et al. ¹¹	N/A
pEX18-pheS-km- <i>Δ</i> ngtA	This paper	N/A
pEX18-pheS-km- <i>Δ</i> ngtA::ngtA	This paper	N/A
pEX18-pheS-km- <i>Δ</i> dptA	This paper	N/A
pEX18-pheS-km- <i>Δ</i> cgaA	This paper	N/A
pEX18-pheS-km- <i>cgaA</i> ^{C97A}	This paper	N/A
pEX18-pheS-km- <i>Tn7::Pnat-cgaA</i>	This paper	N/A
pEX18-pheS-km- <i>cgaA</i> -VSV-G	This paper	N/A
pEX18-pheS-km- <i>cgaA</i> ^{C97A} -VSV-G	This paper	N/A
pEX18-pheS-km- <i>Δ</i> FTN_0433	This paper	N/A
pEX18-pheS-km- <i>Δ</i> ngtA::ngtA ^{LVS}	This paper	N/A
pEX18-pheS-km- <i>Δ</i> ngtA::ngtA ^{SCHU}	This paper	N/A
pEX18-pheS-km- <i>ngtA</i> ^{ΔIGS}	This paper	N/A
pEX18-pheS-km- <i>ngtA</i> -3xFLAG	This paper	N/A
pEX18-pheS-km- <i>Δ</i> ngtA::ngtA ^{LVS} -3xFLAG	This paper	N/A
pEX18-pheS-km- <i>Δ</i> ngtA::ngtA ^{SCHU} -3xFLAG	This paper	N/A
pEX18-pheS-km- <i>ngtA</i> ^{ΔIGS} -3xFLAG	This paper	N/A
pEX18-pheS-km- <i>Δ</i> fupA	This paper	N/A
pMP720	LoVullo et al. ⁶¹	N/A
pMP749	LoVullo et al. ⁶¹	N/A
pMP749- <i>Pbfr-fupA</i>	This paper	N/A
pF	Charity et al. ⁶²	N/A

(Continued on next page)

Continued

REAGENT or RESOURCE	SOURCE	IDENTIFIER
pF- <i>ngtA</i> ^{NOV}	This paper	N/A
pET-28b(+)-6xHis-CgaA	This paper	N/A
pET-28b(+)-6xHis-CgaA ^{C97A}	This paper	N/A
pKL91	Ramsey et al. ¹¹	N/A

Software and algorithms

Geneious Prime 2023.1.2	Geneious, Software, Newark, New Jersey, USA	https://www.geneious.com/ ; RRID:SCR_010519
Prism 9 for macOS	GraphPad, Software, La Jolla, California, USA	https://www.graphpad.com/ ; RRID:SCR_022798
Adobe Illustrator 27.3.1	Adobe Systems Incorporated, San Jose, California, USA	https://www.adobe.com/products/illustrator/ ; RRID:SCR_010279
Chimera version 1.16	UCSF, Software, San Francisco, California, USA	www.rbvi.ucsf.edu/chimera/ ; RRID:SCR_004097

Other

1 mL HisTrap HP column	Cytiva	Cat#17-5247-01
HiLoad 16/600 Superdex 200 pg	Cytiva	Cat#28989335

RESOURCE AVAILABILITY

Lead contact

Further information and requests for resources and reagents should be directed to and will be fulfilled by the lead contact, Joseph Mougous (mougous@uw.edu).

Materials availability

Plasmids and bacterial strains generated in this study are available upon request from the [lead contact](#).

Data and code availability

- Sequence data associated with this study has been deposited to the NCBI Sequence Read Archive: PRJNA967744.
- This paper does not report original code.
- Any additional information required to reanalyze the data reported in this paper is available from the [lead contact](#) upon request.

EXPERIMENTAL MODEL AND STUDY PARTICIPANT DETAILS

Bacterial strains and growth conditions

Bacterial strains used in this study include *Francisella tularensis* subspecies *novicida* U112 (*F. novicida*) and *F. tularensis* subsp. *novicida* MFN245 (*F. novicida* MFN245, both are gifts from Colin Manoil, University of Washington, Seattle, WA), *F. tularensis* subsp. *holarctica* LVS (*F. tularensis* LVS, provided by Karen Elkins, Food and Drug Administration, Rockville, MD), *Escherichia coli* strain DH5 α (*E. coli* DH5 α , Thermo Fisher Scientific), *E. coli* strain BL21 (DE3) (*E. coli* BL21, EMD Millipore). *F. novicida* strains were routinely grown aerobically at 37°C in tryptic soy broth or agar supplemented with 0.1% (w/v) cysteine (TSBC or TSAC). *F. tularensis* LVS was grown aerobically at 37°C in either liquid Mueller-Hinton broth (Difco) supplemented with glucose (0.1%), ferric pyrophosphate (0.025%), and Isovitalex (2%) (MHB) or on cystine heart agar (Difco) supplemented with 1% hemoglobin (CHAH). For selection, antibiotics were used at the following concentrations: kanamycin at 5 μ g/mL (LVS), 15 μ g/mL (U112) or 50 μ g/mL (*E. coli*), carbenicillin at 150 μ g/mL, and hygromycin at 200 μ g/mL. *F. novicida* strains were stored at -80°C in TSBC supplemented with 20% (v/v) glycerol. *E. coli* strains were stored at -80°C in LB supplemented with 15% (v/v) glycerol.

Murine bone marrow-derived macrophage generation

Murine bone marrow-derived macrophages (BMMs) were differentiated from bone marrow of female, 6-12 -weeks-old C57BL/6J mice (Jackson Laboratory) for 5 days in non-tissue culture-treated Petri dishes at 37°C under 10% CO₂ in Dulbecco's Modified Eagle's Medium, containing 1 g/L glucose, L-glutamine and sodium pyruvate (DMEM) supplemented with 10% fetal bovine serum (FBS) and 20% L-929 mouse-fibroblast conditioned medium (L-CSF). 5 days post-plating, non-adherent cells were washed out with ice-cold phosphate buffered saline (PBS) and the differentiated BMMs were incubated for 10 min in ice-cold cation-free PBS (Corning) supplemented with 1 g/L glucose, detached by pipetting and harvested by centrifugation for 7 min at 200xg/ 25°C. Pelleted cells were resuspended in BMM complete medium (DMEM, 10% FBS, 10% L-CSF) and plated at a density of 5x10⁴ cells/ well in 24-well, tissue

culture-treated plates followed by incubation for 48 h at 37°C under 10% CO₂ with replenishment of BMM complete medium at 24 hrs post-plating.

Mice

C57BL/6J mice used in this study were purchased from Jackson Labs. Mice were maintained under SPF conditions ensured through the Rodent Health Monitoring Program overseen by the Department of Comparative Medicine at the University of Washington. All experiments involving mice were performed in compliance with guidelines set by the American Association for Laboratory Animal Science (AALAS) and were approved by the Institutional Animal Care and Use Committee (IACUC) at the University of Washington.

METHOD DETAILS

Strain and plasmid construction

Deletion mutations, *in cis* gene complementation strains, and *in trans* *cgaA* complementation strains of *F. novicida* were generated via allelic exchange as described previously.⁶³ Briefly, sequences containing ~1000 bp flanking the site of deletion or the insertion of the complementation allele (the intergenic site between FTN_0485 and FTN_0486 was used for *cgaA*) were amplified by PCR and cloned into the BamHI and PstI sites of the vector pEX18-pheS-km using Gibson assembly.⁴⁴ Naturally competent *F. novicida* was prepared by back-diluting overnight cultures 1:100 in 2 mL TSBC, growing for 3 hrs at 37°C with shaking, harvesting by centrifugation, and resuspending in 1 mL *Francisella* transformation buffer (per liter; L-arginine, 0.4 g; L-aspartic acid 0.4 g; L-histidine, 0.2 g, DL-methionine, 0.4 g; spermine phosphate, 0.04 g; sodium chloride, 15.8 g; calcium chloride, 2.94 g; tris(hydroxymethyl) amino-methane 6.05 g).⁶³ Approximately 1 μg of pEX18-pheS-km-based deletion or complementation plasmid was added to freshly prepared competent cells. Bacterial suspensions were then incubated at 37°C with shaking for 30 min, followed by addition of 2 mL TSBC and an additional 3 hrs of incubation. Transformants were selected by plating on TSAC with kanamycin. The resulting merodiploids were grown overnight in non-selective TSBC, diluted 1:100 into Chamberlain's defined medium (CDM)⁶⁴ containing 0.1% p-chlorophenylalanine (*w/v*) and allowed to grow to stationary phase. Cultures were then streaked onto TSAC, colonies were patched onto TSAC with and without kanamycin to test for kanamycin sensitivity, and kanamycin sensitive colonies were screened for mutations by colony PCR.

The *fupA* complementation strain ($\Delta fupA$ Tn7:Pbfr-*fupA*) was constructed using the mini-Tn7 system.⁶¹ Briefly, the *fupA* gene was amplified from *F. novicida* by PCR and cloned using Gibson assembly into the pMP749 plasmid along with the sequence encoding the bacterioferritin promoter (Pbfr) for high constitutive expression.^{61,65} Using natural transformation as described above, the resulting plasmid, pMP749-Pbfr-*fupA*, was transformed into plasmid compatible strain *F. novicida* MFN245 carrying the helper plasmid encoding the transposase for Tn7 integration, pMP720. Tn7 integrants were selected on kanamycin, and colonies were screened for the presence of the inserted transposon at the *glmS* locus using PCR. To transfer the Tn7:Pbfr-*fupA* insertion from *F. novicida* MFN245 to *F. novicida* U112, genomic DNA was prepared from Tn7:Pbfr-*fupA* MFN245 strains and 10 ng was used to transform competent U112, prepared as described above. For expressing NgfA^{NOV} in *F. tularensis* LVS, the gene was amplified from *F. novicida* using PCR and cloned into the expression plasmid pF behind the constitutive *groEL* promoter.⁶² Empty pF plasmid or pF-ngfA^{NOV} were electroporated into wild-type or Δggt *F. tularensis* LVS as previously described,⁶⁶ and transformants were selected by plating on CHAH with kanamycin.

For constructing protein expression plasmids pET-28b(+)-6xHis-CgaA or pET-28b(+)-6xHis-CgaA^{C97A}, *cgaA* and *cgaA*^{C97A} were amplified by PCR and cloned into the NdeI and BamHI sites of the vector pET-28b(+) using Gibson assembly

Transposon mutant library generation

Transposon mutant libraries containing 100,000 to 300,000 Mariner transposon insertions in *F. novicida* wild-type and Δggt were constructed using delivery plasmid pKL91.¹¹ The plasmid was delivered via natural transformation as described above, cells were allowed to recover 2 hrs and then plated on TSAC with kanamycin. Plates were incubated for 20 hrs at 37°C and the resulting kanamycin-resistant colonies were scraped and resuspended in CDM broth lacking a cysteine source (CDM-Cys). Each library was washed 4x times with CDM-Cys broth prior to freezing of aliquots containing ~10⁶ CFU each in CDM-Cys with 20% (*v/v*) glycerol at -80°C.

Tn-seq screen

For each genetic background, two aliquots of the respective transposon libraries were thawed and used as the inocula for 50 mL CDM-Cys media. Cultures were placed at 37°C with shaking for 2 hrs prior to addition of 100 μM cysteine or GSH, followed by incubation for 20 hrs at 37°C with shaking. Cells were then collected via centrifugation and genomic DNA was extracted using the DNeasy Blood and Tissue Kit (Qiagen). Sequencing libraries were generated essentially as described.⁶⁷ In brief, 3 μg DNA from each sample was sheared to ~300 bp on a Covaris LE220 Focused-Ultrasonicator followed by DNA-end repair, terminal C-tailing and of amplification of the transposon-genome junctions by two rounds of PCR. The first round employed the transposon-specific primer Fn_TnSeq_1_F and olj376, and second round employed the transposon-specific primer Fn_TnSeq_2_F and distal primer Fn-TnSeq-R2-N701 or Fn-TnSeq-R2-N702 to add unique de-multiplexing barcodes per sample. The libraries were pooled and sequenced using custom sequencing primer Fn_TnSeq-CustomSeq and Read1_SEQ primer by single-end 150 bp sequencing with a single index read on an Illumina MiSeq at 11 pM density with 15% PhiX spike-in.

Tn-seq data processing

Custom scripts^{67,68} (<https://github.com/Ig9/Tn-seq>) were used to process the Illumina sequencing reads and map sites of transposon insertion. First, reads from each sample were filtered for those displaying transposon end sequence (the sequencing primer was designed to anneal five bases from the end of the transposon). The filtered reads were mapped to the genome after removing the transposon end sequence. Reads per unique mapping position and orientation were tallied and read counts per gene were calculated by summing reads from all unique sites within each gene's ORF except those within the 5' 5% and 3' 10% (insertions at gene termini may not be fully inactivating). Gene counts per sample were normalized based on a comparison between all samples of the median reads per gene per gene length for genes with insertions in all samples, as described.⁶⁸

Bacterial growth assays

To examine the proliferation of *F. novicida* on different cysteine sources, strains were first grown overnight in CDM with 57 μM cysteine at 37°C with shaking. Cells were washed three times and resuspended in CDM lacking cysteine (CDM-cys) followed by cysteine starvation for 2 hrs at 37°C with shaking. Cultures were then diluted to an OD_{600} = 0.01 in CDM-Cys supplemented with either GSH, cysteine, or Cys-Gly at 100 μM . Cultures were transferred into a 96-well plate and incubated in a plate reader at 37°C. OD_{600} measurements were taken following a 2 s shake every 10 min. Final growth yields reported represent the OD_{600} obtained after 36 hrs of growth. For *F. tularensis* LVS, strains containing either empty pF plasmid or pF-*ngtA*^{NOV} were first grown overnight in CDM with 1 μM cysteine and then washed and back-diluted to starting OD_{600} = 0.1 in CDM-Cys supplemented with GSH at 100 μM concentration. Cultures were then incubated at 37°C with shaking, and the growth yield was determined by measuring OD_{600} at 16 hrs.

GSH uptake assays

The indicated strains of *F. novicida* were grown to mid-log phase at 37°C in CDM-Cys liquid medium supplemented with 57 μM cysteine. Cells were spun down, washed three times in uptake buffer (25 mM Tris pH 7.5, 150 mM NaCl, 5 mM glucose), then concentrated 20-fold. The OD_{600} was measured and normalized to OD_{600} = 10. Reactions were established containing 20 μL cells, 5 μL 100 μM GSH, 0.5 μCi ³H-GSH ([Glycine-2-³H]-Glutathione, >97%, 50 μCi , PerkinElmer), and 25 μL uptake buffer and incubated for 45 min at 37°C followed by quenching with 1 mL ice-cold uptake buffer. Cells were then pelleted by centrifugation, washed three times in 1 mL cold uptake buffer, then resuspended in 50 μL uptake buffer. Samples were then added to scintillation cocktail (National Diagnostics, Ecoscint Ultra) and counts were measured over 1 minute on a scintillation counter (Beckman, LS6500).

Protein expression and purification

For protein expression, overnight cultures of *E. coli* BL21 carrying pET-28b(+)-6xHis-CgaA or pET-28b(+)-6xHis-CgaA^{C97A} were back diluted 1:500 in 2xYT broth and grown at 37°C until the OD_{600} reached 0.4 ~ 0.6. Protein expression was then induced by the addition of IPTG, and cultures were then incubated with shaking at 18°C for 18 hrs. Following this incubation, cells were collected by centrifugation and resuspended in buffer containing 500 mM NaCl, 50 mM Tris-HCl pH 7.5, 10% glycerol, 5 mM imidazole, 0.5 mg/mL lysosome, 1 mM AEBSF, 10 mM leupeptin, 1 mM pepstatin, 1 mU benzonase, and 5 mM β -mercaptoethanol (BME). Cells were disrupted by sonication and cellular debris was removed by centrifugation at 45,000 x g for 40 min. Lysates were run over a 1 mL HisTrap HP column on an AKTA FPLC purification system to purify the His-tagged proteins. The bound proteins were eluted using a linear imidazole gradient from 5 mM to 500 mM. The purity of each protein sample was assessed by SDS-PAGE and Coomassie brilliant blue staining, and fractions with high purity were concentrated using a 10 kDa cutoff filter. Protein samples were further purified by running over a HiLoadTM 16/600 SuperdexTM 200 pg column equilibrated in sizing buffer (300 mM NaCl, 50 mM Tris-HCl pH 7.5, and 1 mM TCEP). Again, the purity of each fraction was assessed by SDS-PAGE and Coomassie brilliant blue staining. Fractions of the highest purity were pooled, concentrated, and utilized in biochemical assays.

In vitro glutaminase assays

Glutamine amidotransferase activity of purified CgaA and CgaA^{C97A} toward different substrates was assayed in vitro using a glutamate detection kit. 1 μM purified protein was mixed with GSH, glutamine or buffer alone (300 mM NaCl, 50 mM Tris-Cl (pH 8.5)) in 50 μL reactions mixes and incubated 1 hr at 37°C. The reactions were stopped by heating at 95°C for 5 min to inactivate the enzyme. After inactivation, 45 μL of reaction mixtures were added to 100 μL of glutamate detection reaction mix (Abcam Glutamate Assay Kit, ab83389) in a 96-well plate. The reaction mixture was incubated for 5 min at RT followed by 5 min at 37°C. The color change is proportional to the glutamate generated and was measured at A450 in a plate reader. Reported glutamate concentrations were calculated by subtracting background absorbance readings from a no enzyme control.

H₂O₂ sensitivity assays

To monitor H₂O₂ tolerance levels, strains of *F. novicida* were grown at 37°C in CDM medium to mid-log (OD_{600} = 0.4-0.6). Cultures were diluted to an OD_{600} = 0.1 and cell viability was assayed via plating for CFU enumeration. 1.5 mM of H₂O₂ was then added and the cultures were placed at 37°C with shaking. After 30 mins and 60 min, samples were collected for CFU enumeration. Survival rates were calculated by comparing the CFU numbers pre and post-H₂O₂ exposure.

Macrophage infection assays

48 hrs post-plating, BMMs were infected with mid-log phase *F. novicida* at a multiplicity of infection (MOI) of 1 in pre-chilled BMM complete medium. Bacterial uptake was synchronized by centrifugation for 10 min at 400xg/ 4°C after which the plates were immediately placed in a water tray pre-warmed to 37°C and incubated for 30 min at 37°C under 10% CO₂. Following incubation, extra-cellular bacteria were removed by 4 washes with plain DMEM medium pre-warmed to 37°C, the complete BMM medium was replenished, and the plates were placed back at 37°C under 10% CO₂. At 2 hrs and 24 hrs post-infection (p.i.) the BMMs were rinsed 3 times with sterile PBS and lysed in PBS/0.1% sodium deoxycholate (Sigma), followed by serial dilution in sterile PBS and plating on TSAC plates for CFU enumeration. Bacterial growth at 24 h p.i. was normalized to the CFU counts obtained at 2 h p.i.

F. novicida inoculum preparation and intranasal infection

F. novicida inoculum was prepared as described previously.⁶³ Briefly, 3 mL TSBC was inoculated with each *F. novicida* strain and incubated aerobically for 18 h at 37°C with shaking. After overnight growth, cultures were adjusted to OD₆₀₀ = 1 in TSBC, diluted 1:1 with 40% glycerol in TSBC (20% v/v final glycerol concentration), aliquoted and stored at -80°C. The post-freeze titer of each stock was determined by culturing on TSAC. Just prior to infection, an aliquot of each strain was quickly thawed at 37°C and diluted in sterile 1X PBS to ~100 CFU in 30 μL (~3.3 × 10³ CFU/mL).

Mice were infected with indicated *F. novicida* strains by intranasal instillation (30 μL total) under light isoflurane anesthesia. Mice were weighed just prior to and 48 hrs post infection. After 48 hrs mice were euthanized with CO₂. The lungs and spleens were harvested in 5 mL lysis buffer (0.1% IGEPAL, in 1x PBS sterile filtered) and homogenized using a Tissue Teaser Homogenizer (BioSpec Products, Cat# 985370-14). Organ homogenate was serially diluted into 1X PBS and dilutions plated on TSAC. Plates were incubated at 37°C overnight aerobically. Colonies were counted and CFU per organ calculated.

Protein expression level analysis

To analyze the expression of CgaA and CgaA^{C97A} by western blot, *F. novicida* Δ*ggT*, Δ*ggT cgaA*-VSV-G and Δ*ggT cgaA*^{C97A}-VSV-G were grown overnight in CDM with 100 μM cysteine at 37°C with shaking and the equivalent of 1 ml culture at OD₆₀₀=1 was collected for each strain and centrifuged to pellet cells. Cell pellets were resuspended in 50 μL 1x Laemmli buffer,⁶⁹ boiled at 95°C for 5 min, and proteins in 5 μL of each sample were separated by SDS-PAGE. Proteins were then transferred to nitrocellulose membranes, and membranes were blocked in TBST (10 mM Tris-HCl pH 7.5, 150 mM NaCl₂, and 0.05% v/v Tween-20) with 5% (w/v) bovine serum albumin (BSA) for 1 hr at room temperature, followed by incubation with primary antibodies (α-VSV-G with 1:5,000 dilution or α-SodB with 1:20,000 dilution) diluted in TBST with 5% (w/v) BSA for 1 hr at room temperature. Blots were then washed 3x times with TBST, followed by incubation with secondary antibody (Goat α-Rabbit, HRP conjugated, 1:5,000 dilution) diluted in TBST for 1 hr at room temperature. Finally, blots were washed 3x times with TBST, developed using ECL substrate (BIO-RAD), and visualized using the iBright FL1500 Imaging System (Thermo Fisher).

To analyze the expression of NgTA and NgTA variants, *F. novicida* strains Δ*ggT*, Δ*ggT ngtA*-3xFLAG, Δ*ggT ngtA*^{ΔIGS}-3xFLAG, Δ*ggT ngtA*^{SCHU}-3xFLAG, and Δ*ggT ngtA*^{LVS}-3xFLAG were grown to OD ~ 2 in CDM with 100 μM cysteine at 37°C with shaking, pelleted, and resuspended in lysis buffer (150 mM NaCl, 50 mM Tris-HCl pH 7.5, 2% (v/v) Glycerol, 1% (v/v) Triton X-100, 1 mM β-mercaptoethanol, 25 U/mL benzonase, 0.25 mg/mL Lysozyme, and protease inhibitor (cOmplete Protease Inhibitor Cocktail, EDTA-Free, Sigma)). Cells were lysed by sonication (5 rounds, 15 s each) and the resulting cell lysates were clarified by centrifugation at 17,000 rcf for 30 min at 4°C. To concentrate low-abundant NgTA proteins, clarified supernatants were normalized by BCA assay (Thermo Fisher) and equal amounts of protein (5 mg total each sample) were incubated with 40 μL anti-FLAG Affinity Resin (Thermo Scientific) for 4 hrs at 4°C. After incubation, resins were washed 3x times with 1 mL wash buffer (150 mM NaCl, 50 mM Tris-HCl pH 7.5, 2% (v/v) Glycerol, 0.1% (v/v) Triton X-100, 1 mM β-mercaptoethanol) and proteins were eluted by incubating in 2x Laemmli buffer for 30 min at room temperature. Eluted proteins were subjected to western blot analysis as described above with α-FLAG primary antibody (1:800 dilution) and Goat α-Rabbit HRP conjugated secondary antibody (1:5,000 dilution).

NgTA sequence and phylogenetic analysis

To generate a phylogeny, NgTA homologs were identified by collecting the top 5,000 hits from Psi-BLAST, then aligned using the Clustal Omega plug in of Geneious Prime (Dotmatics). Positions with gaps present in at least 30% of sequences were masked in the alignment, and then a neighbor-joining phylogeny was constructed using the Geneious Tree Builder. This phylogeny included both Pht family members and a number of clades of related MFS family proteins from other subfamilies. Non-Pht family clades were eliminated by performing additional BLASTp searches with representatives from each clade that did not contain a previously characterized Pht family member; clades were eliminated when these sequences had higher percent identity matches with other MFS transporter families than with the closest Pht family member. This yielded a set of 1,043 sequences that were re-aligned and masked as described above, and used to construct a new neighbor joining phylogeny.

Inactivating mutations in *ngtA* coding sequences were identified by performing a tBLASTn search with NgTA, limited to the Thio-trichales. All protein sequences obtained were filtered to remove those sharing <50% identity with NgTA of *F. novicida*, as these were found to represent other Pht family members. Remaining protein sequences were then aligned. In cases where a premature stop codon had been introduced into the coding sequence of *ngtA*, our tBLASTn search retrieved multiple hits, which manifested as truncated sequences in the protein sequence alignment. For *F. endociliophora*, the absence of *ngtA* was confirmed by performing a

BLASTp search with NgtA against the complete genome, and by examining the conserved genomic location where *ngtA* is encoded in other strains.

QUANTIFICATION AND STATISTICAL ANALYSIS

Statistical significance in bacterial growth assays, GSH uptake assays, *in vitro* glutaminase assays, and H₂O₂ sensitivity assays was assessed by unpaired two-tailed student's t-test between relevant samples. Statistical significance in macrophage infection assays and mouse infection assays was assessed by one-way ANOVA with Dunnett's multiple comparison test comparing mutant strains to wild-type. Details of statistical significance is provided in the figure legends.